PRESSURE-INDUCED INFRARED ABSORPTION OF THE FUNDAMENTAL BAND OF DEUTERIUM IN D_2-He AND D_2-Ne MIXTURES AT DIFFERENT TEMPERATURES

WILSON E. RUSSELL

PRESSURE-INDUCED INFRARED ABSORPTION OF THE FUNDAMENTAL BAND OF DEUTERIUM IN D_2-He AND D_2-Ne MIXTURES AT DIFFERENT TEMPERATURES

by

© Wilson E. Russell, B.Sc.

Submitted in partial fulfilment
of the requirements for the degree of Master of Science
Memorial University of Newfoundland

January, 1968

This thesis has been examined and approved by:

Professor (Miss) E. J. Allin, M.A., Ph.D.

Department of Physics

University of Toronto

and

Professor T. T. Gien, M.Sc., Ph.D.

Department of Physics

Memorial University of Newfoundland

CONTENTS

ABSTRACT

The pressure-induced fundamental infrared absorption band of deuterium in D_2-He mixtures at 77°K, 201°K and 273°K and in D_2-Ne mixtures at 77°K, 201°K, 273°K and 298°K was studied for gas pressures up to 600 atm for different base pressures of deuterium. The shapes of the enhancement absorption contours obtained in each case were discussed. The contours for D_2-He mixtures showed the splitting of the Q branch with the components Q_P and Q_R, the splitting being more pronounced at the higher temperatures. The quadrupolar lines S(0) and S(1) which appeared distinctly in the contours for D_2-Ne mixtures at 77°K were found to be absent in the corresponding contours for the D_2-He mixtures. Integrated absorption coefficients were measured and the binary and ternary absorption coefficients were derived. The theory of the "exp-4"model was applied to the binary absorption coefficients obtained experimentally. The quadrupolar parts of the binary absorption coefficients were calculated from the known molecular parameters and were then subtracted from the experimental values to obtain the overlap parts. The two overlap parameters λ and ρ, giving respectively the magnitude and the range of the overlap moment, were determined for each of the mixtures by fitting the calculated overlap part of the binary absorption coefficient as a function of the temperature to the experimental values of the overlap parts using a method of successive trials.

INTRODUCTION

1.1 Pressure-Induced Absorption of the Infrared Fundamental Band of Gaseous Deuterium

Soon after the discovery of rotation-vibration infrared absorptions by intermolecular forces in liquid and compressed oxygen and in compressed nitrogen by Crawford, Welsh and Locke (1949), the fundamental infrared absorption band of hydrogen aroused much interest among researchers particularly among Welsh and his collaborators at McLennan Laboratory, University of Toronto. Over the years the band has been studied very extensively in gaseous, liquid and solid phases of hydrogen under a variety of experimental conditions (for references, see Lee 1967). However, such detailed experimental studies are not available for the fundamental infrared absorption band of deuterium until recently. A preliminary study of the band in the gaseous phase was made first by Chisholm (1952). A detailed investigation of this band was made at room temperature by Reddy and Cho (1965a) in the pure gas at pressures up to 250 atm and by Pai, Reddy and Cho (1966) in D_2-He, D_2-A, and D_2-N_2 mixtures at pressures up to 1200 atm. These measurements of the induced absorption in pure deuterium and deuterium-foreign gas mixtures showed that the integrated absorption coefficient of the fundamental band of deuterium in the pure gas and enhancement in the integrated absorption coefficient of the same band in the mixtures are density-dependent according to the following relations:

For the pure gas,

$$\int \alpha(\nu)d\nu = \alpha_{1a}\rho_a^2 + \alpha_{2a}\rho_a^3$$

and for the mixtures,

$$\int \alpha_{en}(\nu)d\nu = \alpha_{1b}\rho_a\rho_b + \alpha_{2b}\rho_a\rho_b^2 .$$

Here ρ is the density in Amagat units, suffix a refers to the absorbing gas, and suffix b to the perturbing gas. α_{1a} and α_{1b} are binary absorption coefficients which arise due to binary collisions, and α_{2a} and α_{2b} are ternary absorption coefficients which occur as a result of ternary collisions. These relations are similar to those that described the integrated absorption coefficients of the induced absorption of the fundamental band of hydrogen. Watanabe and Welsh (1965) studied the band in pure deuterium gas at low pressures in the temperature range 24°K to 77.3°K and obtained the evidence for the existence of the bound states of the $(D_2)_2$ complex. Very recently a preliminary study of this band in the pure gas and in D_2-He and D_2-Ne mixtures at low temperatures has been made by Sinha (1967). In the studies of the band at room temperature and at intermediate temperatures, the absorption profiles were found to exhibit a splitting of the Q branch into two well-resolved components, with the minima occurring at the band origin ν_o. The higher and lower frequency components are referred to as the Q_R and Q_P components respectively.

According to Condon's theory (1932), the dipole moment induced in a molecule by a static electric field gives rise to transitions which obey the Raman rather than the infrared selection rules. In the absorption induced by intermolecular forces, the polarization of the absorbing molecule by a perturbing molecule during a collision would produce a similar effect. Accordingly, the intensity distribution for the induced infrared absorption of the fundamental bands of homonuclear diatomic gases was found to obey

the Raman selection rules for rotation, i.e., ΔJ = -2(O branch), O(Q branch), and +2(S branch), where J is the rotational quantum number. To illustrate possible single transitions between the lower and upper rotational levels for the fundamental vibration absorption band of deuterium (i.e., v' = 1, J' ← v" = o, J"), a schematic energy level diagram is presented in Fig. 1. Here, the vibrational spectral terms $G_0(V)$, the rotational spectral terms $F_V(J)$ and the frequencies of different transitions are calculated from the molecular constants of deuterium determined from the high resolution Raman spectrum of gaseous deuterium at room temperature by Stoicheff (1957). The relative population, N_J, of deuterium molecules at any temperature can be calculated from (i) the Boltzmann distribution law, (ii) the (2J+1)-fold degeneracy of the rotational levels, and (iii) the degeneracy of the rotational levels due to nuclear spin. The degeneracy due to nuclear spin is calculated as follows. Since the nuclear spin, I, of a deuterium atom is 1, the total nuclear spin, T, of a deuterium molecule takes the values 2(parallel spins), 1 (inclined spins) and 0 (antiparallel spins). Even T values are possible for symmetric levels (J = 0,2, 4, ----) and odd T for antisymmetric levels (J=1, 3, 5, ----). A rotational energy level with a given value of T has a statistical weight 2T+1 which gives the statistical weights 6 (5 (corresponding to T=2) + 1 (corresponding to T=0)),and 3, for the even and odd rotational levels respectively. Since the pressure-induced absorption originates from molecular collisions, the individual transitions give rise to very broad lines giving a characteristic broad appearance for the band.

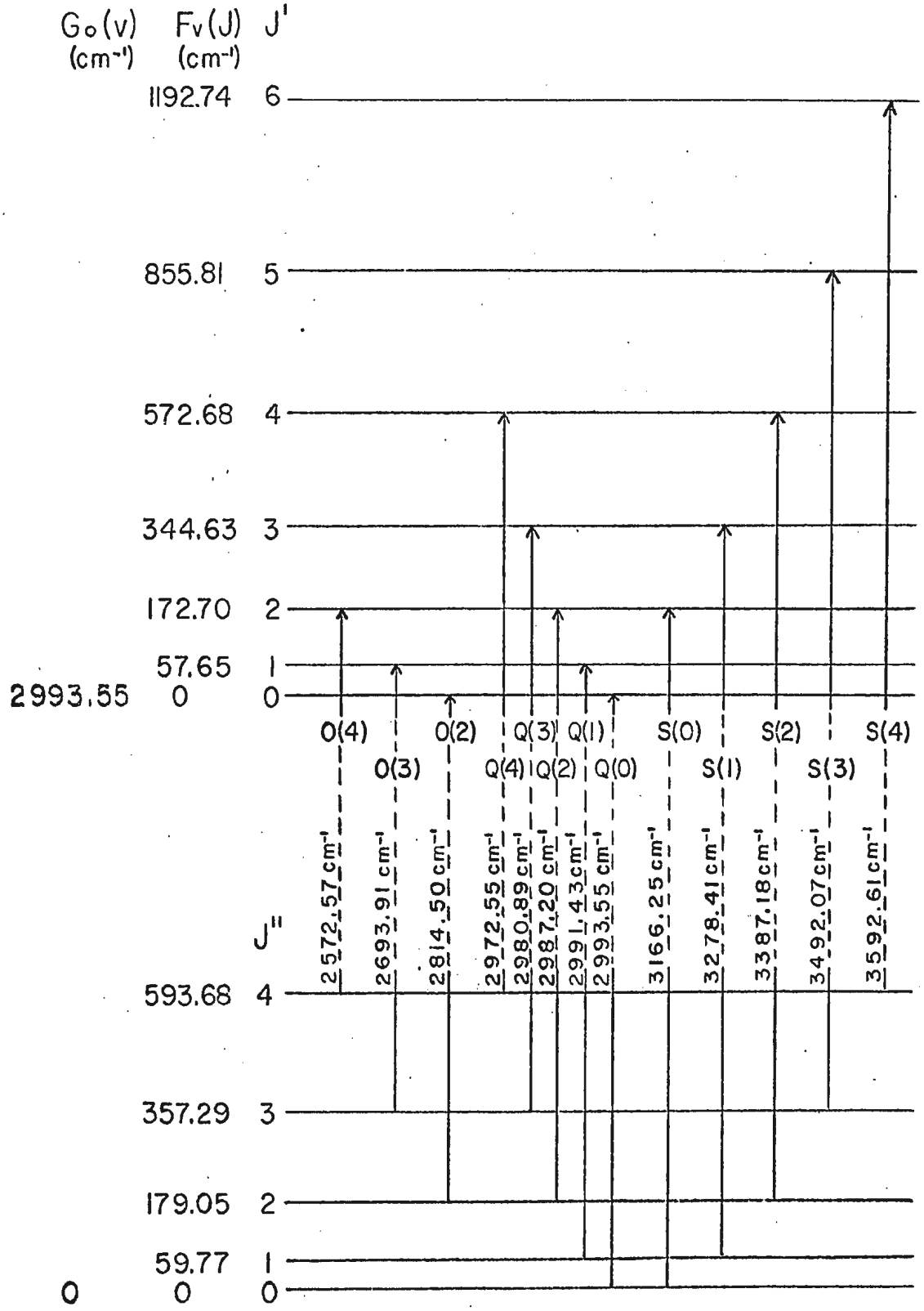

Fig. 1. Energy level diagram of the induced fundamental band of deuterium.

1.2 A Brief Outline of the Theory of the Pressure-Induced Absorption

A detailed summary of the theory of the pressure-induced absorption of the fundamental bands of homonuclear diatomic molecules is given in the Appendix. According to the theory given by Van Kranendonk (1957, 1958), the induced dipole moment in a binary collision between an absorbing symmetric diatomic molecule and a perturbing molecule consists of two additive parts. One of these is the angle-independent short-range electron overlap dipole moment which decreases exponentially with the intermolecular distance, R, and mainly contributes to the intensity of the Q branch. The other part is the angle-dependent long-range dipole moment resulting from the polarization of one molecule by the quadrupole field of the other and is proportional to R^{-4}. This contributes to the intensity of the O, Q and S branches. The quadrupolar contribution to the Q branch is referred to as the Q_Q component. The theory mentioned here is often referred to as the theory of the (exp-4) model in which the short-range overlap moment is determined by two overlap parameters λ and ρ, giving respectively the magnitude and the range of the moment. The long-range quadrupole moment is usually calculated using the known molecular parameters. The parameters λ and ρ can be determined by fitting the theoretical binary absorption coefficient as a function of the temperature to the experimental values of the binary absorption coefficient. The temperature dependence of the absorption coefficient is determined mainly by ρ while its magnitude is determined by λ. A preliminary value of λ can be obtained first by assuming a reasonable value for ρ and fitting the calculated binary absorption coefficient at a given temperature to the experimental value. This value

of λ is used to calculate the binary absorption coefficients at other temperatures, which are then compared with the experimental values at the corresponding temperatures. This procedure is repeated for some more reasonable values for ρ until the experimental and theoretical curves for the variation of the binary absorption coefficient with the temperature agree very closely.

1.3 The Present Investigation

The present investigation was designed to obtain new information on the pressure-induced fundamental infrared absorption band of deuterium using helium and neon as perturbers. Since the polarizabilities of helium and neon are small the main contribution to the binary absorption coefficients comes from the overlap parts (up to 80 to 90% approximately). It was expected that the variation of the overlap part of the binary absorption with the temperature could be studied more accurately in the present investigation. The band was studied in D_2-He and D_2-Ne mixtures for gas pressures up to 600 atm and temperatures in the range 77°K to 298°K. The shapes of the experimental contours were discussed. Integrated absorption coefficients were measured and the binary and ternary absorption coefficients were derived for the fundamental band in each of the mixtures at the experimental temperatures. The data for D_2-He mixtures at 298°K were supplemented from Pai, Reddy and Cho (1966). The theory of the "exp-4" model of Van Kranendonk (1958) has been applied to the experimental values of the binary absorption coefficients. By subtracting the quadrupolar parts of the binary absorption coefficients, calculated from the known molecular parameters, from their experimental values, the overlap parts were obtained. The two overlap

parameters λ and ρ, giving respectively the magnitude and range of the overlap moment, were determined for each of the mixtures by fitting the calculated overlap part of the binary absorption coefficient as a function of the temperature to the experimental values of the overlap parts using a method of successive trials.

CHAPTER 2

EXPERIMENTAL PROCEDURE

This chapter contains a description of the experimental apparatus and procedure used in the study of the pressure-induced fundamental band of deuterium in D_2-He and D_2-Ne mixtures in the temperature range from 77°K to 298°K and at pressures up to 600 atm. In the present investigation, the fundamental band has been studied in D_2-He mixtures at 77°K, 201°K, and 273°K, and in D_2-Ne mixtures at 77°K, 201°K, 273°K, and 298°K.

2.1 The High Pressure Gas Absorption Cell

The absorption cell (Fig. 2) was of the transmission type having an optical path length of 25.8 cm at room temperature. The details of its design have been described by Sinha (1967). The body of the cell, A, 15.5 in. long, 3.2 in. in diameter, has a central bore of 3/4 in., and was constructed of type No. 303 stainless steel. The stainless steel light guide, G, made in two sections, and having a central rectangular aperture, 3/8 in. x 3/16 in., was fitted into the bore of the cell body. The inner surface of the light guide was polished so that reflection, and hence, transmission, of radiation would be good. The entrance and exit windows, W, were polished synthetic sapphire plates, 5 mm in thickness and 1 in. in diameter. These windows were cemented on to the window plate holders, P, by means of General Electric silicone rubber cement. Steel caps, C, with teflon washers, D, between the caps and the window to prevent chipping, held the windows in place during evacuation of the cell. The apertures in the window plates were of the same dimensions as the aperture in the light guide. These apertures were designed to allow a f/4 cone of radiation

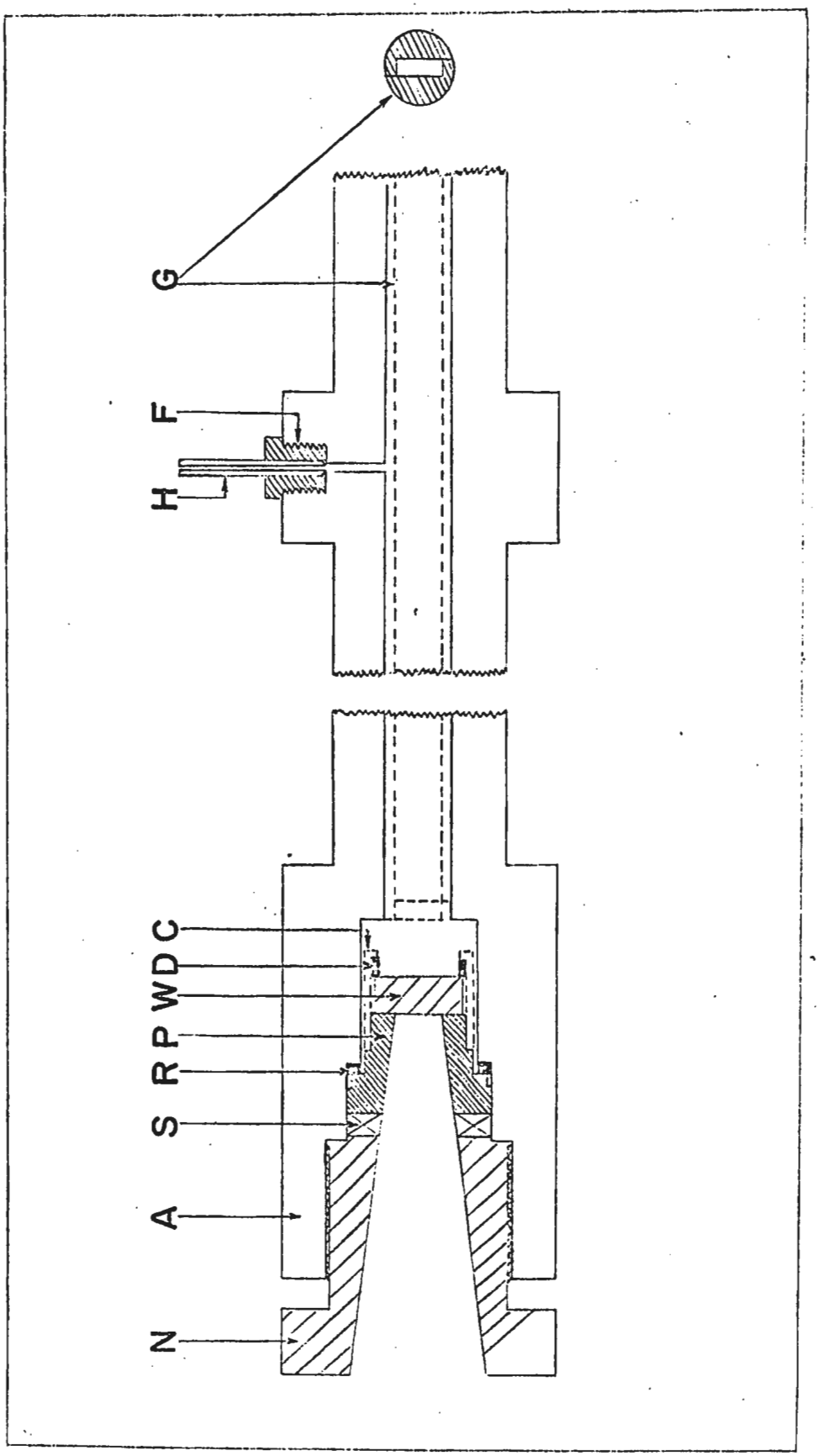

Fig 2. High pressure gas absorption cell

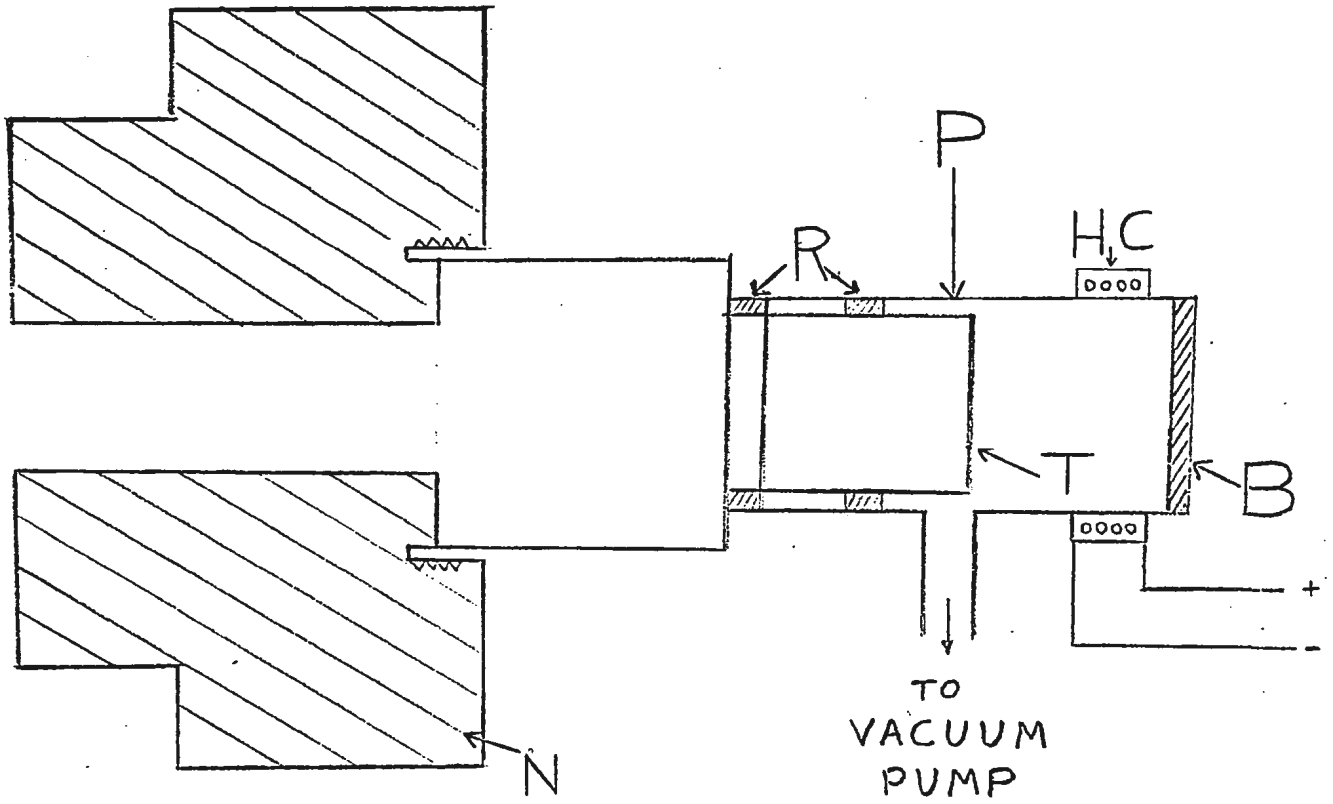

Fig. 3. End-pieces attached to the cell for low temperature experiments.

to focus the source and spectrometer slit on the entrance and exit ends of the cell, respectively. The section, S, of the window plates, 0.35 in. in thickness, was made square and fitted exactly into a square recess in the cell body. This prevented non-alignment of the apertures in the window plates with the one in the light guide when the hexagonal stainless steel closing nuts, N, were tightened. Invar rings, R, 1/8 in. thick, between the window plates and the cell body gave a good pressure seal after the nuts, N, were tightened. The gas entered the cell through a steel capillary tube, H, of diameter 1/4 in., connected to the center of the cell by means of an Aminco-fitting, F. The cell was pressure-tested up to 1200 atm at room temperature (298^{o}K) and up to 400 atm at liquid nitrogen temperature (77^{o}K).

For experiments at temperatures 273^{o}K and below, the absorption cell had an outer jacket in which the coolant was kept. The coolants used in this study were crushed ice (273^{o}K), alcohol-dry ice mixture (201^{o}K), and liquid nitrogen (77^{o}K). To prevent condensation on the windows of the cell at these temperatures, end-pieces, P, made of plexiglass and shown diagramatically in Fig. 3, could be evacuated. These end-pieces were fitted vacuum-tight by means of rubber O-rings, R, over steel extension tubes, T, cemented into the hexagonal nuts, N. Heater coils, HC, through which a current of 0.7 amp was passed, prevented condensation from forming on the outer windows, B, which were optically flat synthetic sapphire plates, 1 in. in diameter and 2 mm thick, and were cemented on to the end-pieces, P, by means of General Electric silicone rubber cement.

The optical path length of the cell was 25.8 cm at 298^{o}K and 273^{o}K, and 25.7 cm at 201^{o}K and 77^{o}K.

2.2 The Optical System

The optical arrangement used in the present experiments is shown in Fig. 4. The experiments were performed with a Perkin-Elmer Model 112 double pass spectrometer, A, using a LiF prism and a Unican Pneumatic Golay Detector, G. The infrared-radiation source, S, was a water-cooled globar, operating by means of a stabilized power supply from an electronic source radiation controller. The source and the controller were supplied by the Warner and Swasey Co., Flushing, N.Y. The controller was fed by a Sorenson A.C. regulator, Model ACR-2000.

Radiation from the source was first reflected by an aluminized spherical front surface mirror, M_1, with a radius of curvature 15.9 in. Then it passed through the absorption cell, H, and was reflected and focused by an identical mirror, M_2, onto the entrance slit, S_1, of the double pass spectrometer, A. This entrance slit was kept at 500 μ, which gave a spectral resolution of ~ 13 cm^{-1} at 2994 cm^{-1}, the origin of the fundamental band of deuterium. A f/4 light cone was used throughout the external optical arrangement in order to match the internal optics of the spectrometer. The spectral region from 2500 cm^{-1} - 3750 cm^{-1} was calibrated using known frequencies of absorption peaks of the atmospheric water vapour (Perkin-Elmer spectrometer instruction manual, Vol. 3A), and liquid indene (I.U.P.A.C. Tables of Wavenumbers, 1961).

2.3 The Experimental Method

The high pressure gas system is shown schematically in Fig. 5. G_1, G_2, G_3, and G_4 are Bourdon-type pressure gauges. C is a mercury-column gas compressor. H is the gas absorption cell. V_1 to V_8 are Aminco needle valves.

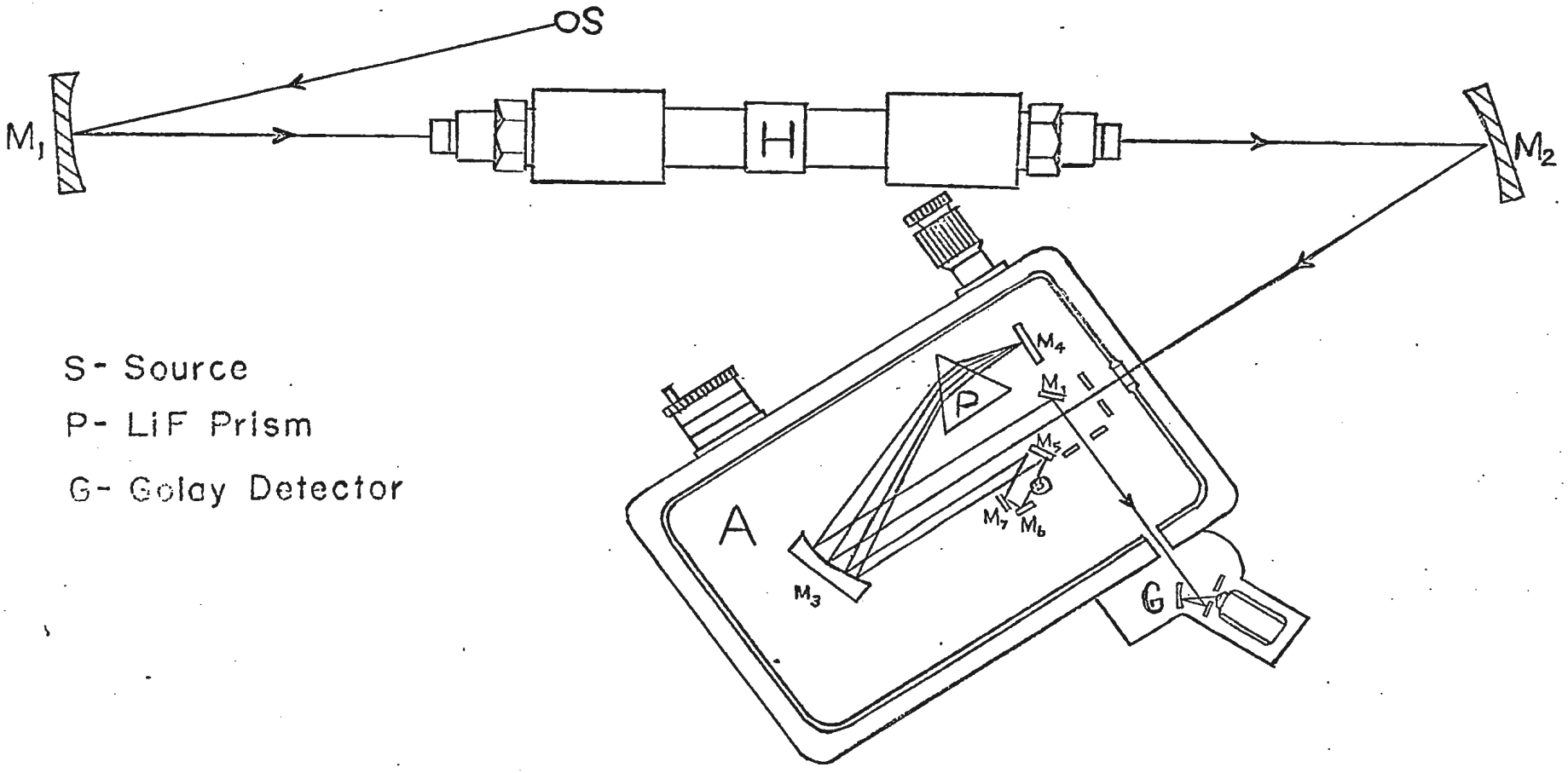

Fig. 4. The optical arrangement.

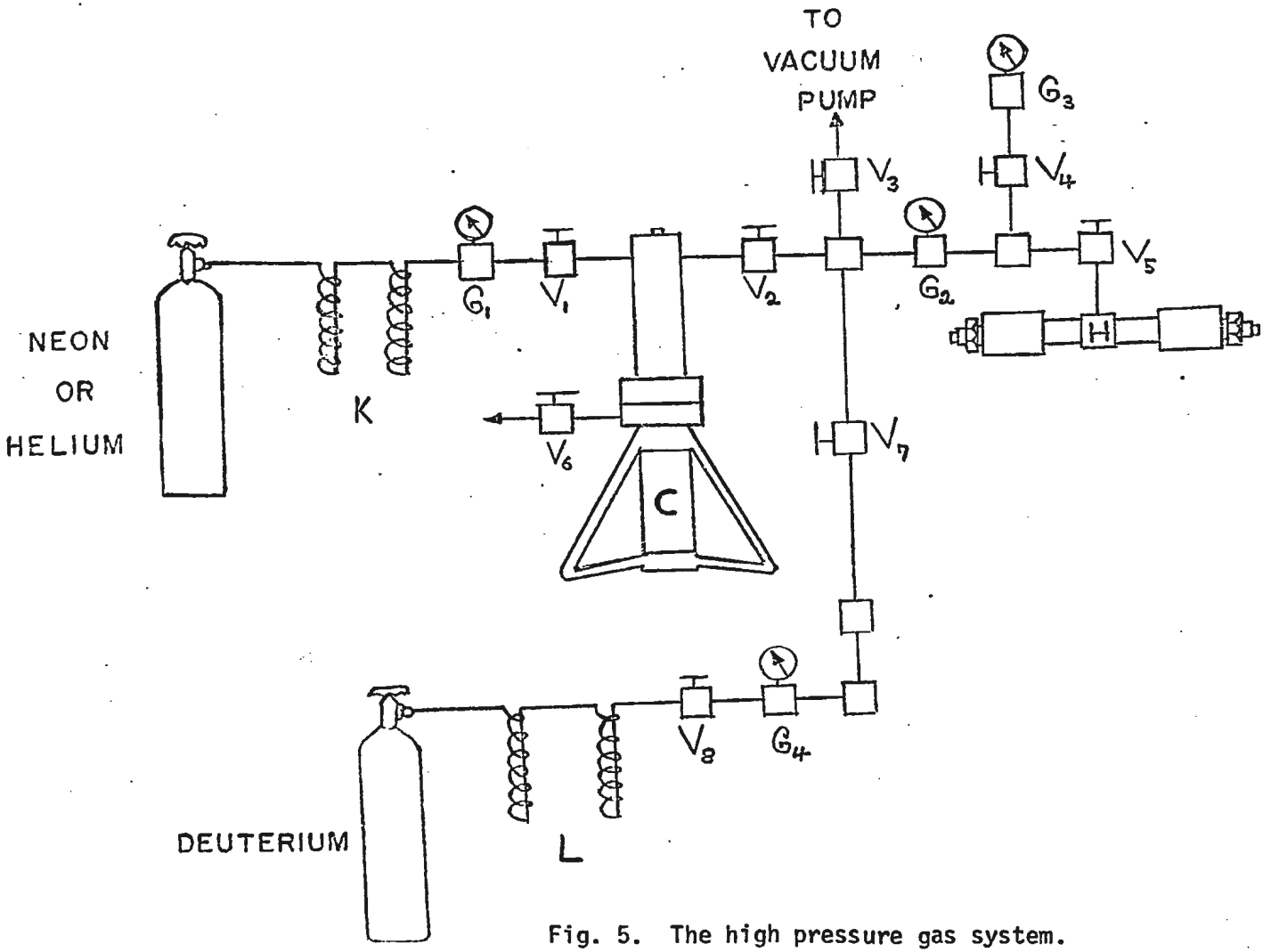

Fig. 5. The high pressure gas system.

The connections between the different components were made by stainless steel capillary tubing with 1/4 in. outside diameter. The length of the tubing between valve, V_5, and the absorption cell was made short in order to reduce the error caused by the deuterium contained in that section. This system was tested for pressures up to 800 atm for several days and for vacuum down to a pressure of ~ 0.1 mm of mercury for several hours.

D_2-Ne Experiments at 298°K:

Before the beginning of an experiment, the afore-mentioned system was evacuated for several hours. Then, with the valves, V_3, V_2, and V_1, closed, the valves, V_8, V_7, V_4, and V_5, were opened. Deuterium gas from a commercial cylinder, supplied by Matheson of Canada, Ltd., Whitby, Ontario, was allowed to pass through the liquid nitrogen traps, L, of 1/4 in. diameter copper tubing, and into the absorption cell. The pressure reading of this deuterium base was made on the 0-1000 p.s.i. gauge G_3. The valve, V_5, was then closed and recorder traces of the absorption spectrum were taken until a satisfactory reproduction was obtained. Then, with the valves, V_5 and V_8, kept closed, the rest of the high-pressure system other than the absorption cell was evacuated. The valves, V_3 and V_4, were then closed. Neon gas from a commercial cylinder, also supplied by Matheson of Canada, Ltd., was allowed to enter the gas compressor through valve, V_1, after passing through the purifying liquid nitrogen traps, K, of 1/4 in. diameter copper tubing. Valve, V_1, was then closed and the neon gas was compressed by a column of mercury in the compressor driven by an Aminco hand-operated oil pump. The neon gas was then admitted in pulses into the absorption cell by opening and closing the valve, V_5, quickly several times, thus preventing

back diffusion of the deuterium gas already in the cell. When the pressures on both sides of the valve, V_5, were equalized, the pressure was read on the 0-10,000 p.s.i. gauge, G_2. To test the completion of the mixing of deuterium and neon in the absorption cell, the spectrometer was set beyond the absorption region of the fundamental band of deuterium. The mixing was assumed to be complete when the recorder pen deflection, which fell off during the sudden admission of the foreign gas, came back to its original level. This usually took ~ 15 minutes. Recorder traces of the absorption spectrum were then taken until a satisfactory reproduction was obtained. Base pressures of deuterium of 40 atm and 45 atm were used for the experiments at 298°K with neon as the perturbing gas.

D_2-He and D_2-Ne Experiments at 77°K, 201°K, and 273°K:

For D_2-He and D_2-Ne experiments at temperatures 77°K, 201°K, and 273°K, the plexiglass end-pieces fitted with sapphire windows, mentioned previously, were attached to the ends of the absorption cell. For these experiments, the procedure was much the same as the procedure for the D_2-Ne experiments at 298°K. The coolants were liquid nitrogen, alcohol-solid carbon dioxide mixture, and ice, for the experiments at 77°K, 201°K, and 273°K, respectively. The absorption cell was completely enveloped by these coolants, contained in the outer jacket of the cell. The temperature of the cell was read on a thermometer with a range of 73°K - 300°K which was placed touching the cell. The same method, described above, was used for admitting the gases into the absorption cell. It was noted that the recorder pen deflection, which fell off on admission of the foreign gas,

took ~ 30 minutes to return to its original level. At these temperatures, base pressures of deuterium ranging from 14 atm to 44 atm were used for the experiments with neon as the perturbing gas, and base pressures ranging from 17 atm to 54 atm were used for the experiments with helium as the perturbing gas. During these experiments, the pen deflection for infinite absorption (i.e. for zero radiation entering the spectrometer) was checked several times.

2.4 Reduction of Experimental Traces

As we were mainly interested in the enhancements in absorption of the fundamental band of deuterium when a foreign gas was admitted, at a series of pressures, into the absorption cell containing a fixed base pressure of deuterium, the recorder traces obtained in an experiment for several pressures of the mixture were plotted on the recorder trace obtained with the corresponding pure deuterium base. Water absorption peaks which occurred at the high frequency end of the deuterium fundamental band were used for matching. Then the base trace was placed over the frequency calibration trace using the water absorption peak at 3732 cm^{-1} for matching. The traces were reduced by means of a logarithmic scale that gave $\log_{10}(I_1/I_2)$ from which the absorption coefficient, $\alpha_{en}(\nu)$, was determined. $\alpha_{en}(\nu)$ is defined by Beer's Law

(1) $$I_2 = I_1 \exp(-\alpha_{en}(\nu)\ell)$$

or

(2) $$\alpha_{en}(\nu) = \frac{2.303}{\ell} \log_{10}(I_1/I_2)$$

where I_1 is the intensity of radiation transmitted at a frequency, ν, by

the pure deuterium base in the absorption cell of optical path length, ℓ, I_2 is the intensity of radiation transmitted by a deuterium-foreign gas mixture in the cell at the same frequency, ν, and $\alpha_{en}(\nu)$ is the enhancement in the absorption coefficient. Values of $\log_{10}(I_1/I_2)$ were read at frequency intervals of 10 cm^{-1} across the band. The enhancement absorption profiles were obtained by plotting $\log_{10}(I_1/I_2)$ against frequency in cm^{-1}.

2.5 Isothermal Data of Gases at Different Experimental Temperatures

The densities of the gases used in the experiments were expressed in units of Amagat which is the ratio of the density of a gas at a given temperature and pressure to its density at standard temperature and pressure (i.e. S.T.P.).

DEUTERIUM:

The pressure-density (P-ρ) relations of deuterium gas at 298°K and 273°K were obtained directly from the isothermal data of Michels and Goudeket (1941).

The densities of deuterium at 201°K were calculated from the available isothermal data of Michels et al (1959) for deuterium at 198°K and 223°K by the method of linear interpolation.

The densities of deuterium at 77°K were obtained from the data compiled by Sinha (1967) who calculated the isothermal data up to 49 atm, directly from the data available for hydrogen in NBS Technical Note 120 by Dean (1961) using the procedure outlined on page 434 of NBS RP 1932 by Woolley, Scott and Brickwedde (1948). According to this procedure the actual density of deuterium D_{2P} in Amagat units can be expressed as

(3) $$D_{2P} = H_{2P} \times (Z_H/Z_D)$$

where H_{2P} is the actual density of hydrogen in Amagat units, $Z_H = PV/RT = (1 + BP + CP^2)$ is the compressibility factor for hydrogen, and Z_D is the compressibility factor for deuterium. Up to 165 atm, the isotherms for deuterium were also calculated by Sinha by a similar method using the available data for hydrogen given by Woolley, Scott and Brickwedde (1948). Beyond 165 atm, the isotherms were calculated from the best polynomial fit of the equation of state

(4) $PV = RT\ (1 + BP + CP^2)$.

The most suitable values of B and C were found to be $B = -817 \times 10^{-6}\ (atm)^{-1}$ and $C = +110 \times 10^{-7}\ (atm)^{-2}$. The isothermal data of deuterium at 201°K and 77°K are summarized in Table I.

HELIUM:

The isotherms of helium gas at 273°K, 201°K, and 77°K, up to a pressure of 100 atm, were directly derived from the data from the NBS Technical Note by Mann (1962). The isothermal data of helium at 273°K and 201°K above 100 atm were determined using the equation (see the American Institute of Physics Handbook, 1963),

(5) $PV = A_1 + B_1 \rho_A + C_1 \rho_A^2$

where ρ_A is the density in Amagat units and V is the molar volume, defined as the ratio of the molecular weight, M, to the usual density, d. From equation (5) we obtain the equation

(6) $P = Ad + Bd^2 + Cd^3$

where A, B, and C are constants.

TABLE I

Isothermal data for deuterium

p (Atmospheres) At 201°K	ρ (Amagat) At 201°K	p (Atmospheres) At 77°K	ρ (Amagat) At 77°K	p (Atmospheres) At 77°K	ρ (Amagat) At 77°K
10.0	13.26	1.69	6.00	83.42	300.06
20.0	26.34	2.82	10.00	89.85	320.06
30.0	39.89	5.61	20.01	103.55	360.05
40.0	53.02	11.13	40.01	118.59	400.05
50.0	65.62	16.58	60.02	135.33	440.05
60.0	78.40	21.97	80.02	154.13	480.06
70.0	90.72	27.37	100.09	164.43	500.06
80.0	102.98	32.66	120.02	200.0	553.50
90.0	115.11	37.99	139.96	240.0	589.85
100.0	126.84	43.34	159.96	280.0	605.55
110.0	138.66	48.79	180.15	300.0	607.43
120.0	150.11	54.20	200.03	320.0	606.21
130.0	161.45	59.76	218.73	340.0	602.47
140.0	172.56	65.43	240.03	-	-
150.0	183.35	71.25	260.26	-	-
160.0	193.65	77.24	279.86	-	-

The P-d relations were then calculated from the best polynomial fit of equation (6). The most suitable values for helium at 273°K were found to be $A = 5.596 \times 10^3$ atm - (cc/gm), $B = 2.047 \times 10^4$ atm - $(cc/gm)^2$, and $C = 6.801 \times 10^4$ atm - $(cc/gm)^3$.

The most suitable values of A, B, and C for helium at 201°K were found to be $A = 4.118 \times 10^3$ - (cc/gm), $B = 1.481 \times 10^4$ atm - $(cc/gm)^2$, and $C = 4.201 \times 10^4$ atm - $(cc/gm)^3$.

Beyond 100 atm, the isothermal data of helium at 77°K were taken from the compiled data of Sinha (1967), calculated using the best polynomial fit of the equation of state (4). The most suitable values for B and C for helium at 77°K were found to be $B = +1.803 \times 10^{-3}$ $(atm)^{-1}$ and $C = +0.5167 \times 10^{-6}$ $(atm)^{-2}$.

The calculated isothermal data of helium are summarized in Table II.

NEON:

The isothermal data for neon at 298°K was obtained directly from Michels, Wassenaar, and Louwerse (1960).

The densities of neon at 273°K, 201°K, and 77°K for pressures up to 200 atm, were determined by a linear interpolation method from the available data of Timmerhaus (1963). The isothermal data for neon at 273°K and 201°K above 200 atm were determined from equation (6). The most suitable values for A, B, and C for neon gas at 273°K were found to be $A = 1.113 \times 10^3$ atm - (cc/gm), $B = 4.738 \times 10^2$ atm - $(cc/gm)^2$, and $C = 1.255 \times 10^3$ atm - $(cc/gm)^3$.

The most suitable values for A, B, and C for neon at 201°K were found to be $A = 8.186 \times 10^2$ atm - (cc/gm), $B = 2.799 \times 10^2$ atm - $(cc/gm)^2$, and $C = 7.973 \times 10^2$ atm - $(cc/gm)^3$.

TABLE II

Isothermal data for helium

P (Atmospheres) At 273°K	ρ (Amagat)	P (Atmospheres) At 273°K	ρ (Amagat)	P (Atmospheres) At 273°K	ρ (Amagat)
1.0	1.00	100.0	94.04	307.3	257.6
5.0	5.00	107.7	100.8	339.5	280.0
10.0	9.95	120.6	112.0	389.5	313.6
20.0	19.77	133.7	123.2	441.9	347.1
30.0	29.46	147.0	134.4	496.9	380.7
40.0	39.04	160.5	145.6	553.8	414.3
50.0	48.49	174.3	156.8	613.5	447.9
60.0	57.83	188.1	168.0	676.0	481.5
70.0	67.05	216.7	190.4	726.0	515.1
80.0	76.15	245.9	212.8		
90.0	85.15	276.7	235.2		

TABLE II (Continued)

Isothermal data for helium

P (Atmospheres) At 201°K	ρ (Amagat)	P (Atmospheres) At 201°K	ρ (Amagat)	P (Atmospheres) At 201°K	ρ (Amagat)
1.0	1.36	100.0	125.24	236.4	268.8
5.0	6.76	107.9	134.4	260.1	291.2
10.0	13.47	117.8	145.6	284.4	313.6
20.0	26.72	129.1	156.8	309.5	336.0
30.0	39.74	138.0	168.0	348.5	369.5
40.0	52.57	148.4	179.2	389.0	403.1
50.0	65.16	158.8	190.4	431.2	436.7
60.0	77.56	169.4	201.6	475.3	470.3
70.0	89.75	180.2	212.8	521.2	503.9
80.0	101.77	191.1	224.0	601.9	559.9
90.0	113.59	213.5	246.4		

The calculated isothermal data of neon are summarized in Table III.

2.6 Determination of the Partial Density of a Foreign Gas in a Binary Gas Mixture

The partial density, ρ_b, of a foreign gas in a binary gas mixture was obtained by using the interpolation formula

$$\rho_b = \frac{1}{1+\beta^1} \left[(\rho_a)_P + \beta^1 (\rho_b)_P \right] - \rho_a$$

where ρ_a is the density of the deuterium base, $(\rho_a)_P$ and $(\rho_b)_P$ are the densities of deuterium and the foreign gas, respectively, at the total pressure, P, of the mixture, and $\beta^1 = \rho_b{}^1/\rho_a$ where $\rho_b{}^1$ is the approximate partial density of the foreign gas.

This approximate interpolation method was used by Cho, Allin and Welsh (1963) and Reddy and Cho (1965) and was shown to be accurate within the range of the experimental error.

2.7 A Note on the Ortho-Para Conversion of Deuterium Contained in a Steel Cell at Low Temperatures

In contrast to molecular hydrogen, ortho-deuterium molecules exist in even rotational levels (J = 0, 2, 4, ----) and para molecules in odd levels (J = 1, 3, 5, ----). In normal deuterium, the ratio of ortho and para concentrations is 2:1. In experiments at liquid nitrogen temperature using a steel absorption cell, Sinha (1967) observed in our laboratory that no detectable conversion had taken place within the period of an

TABLE III

Isothermal data for neon

p (Atmospheres) At 273°K	ρ (Amagat) At 273°K	p (Atmospheres) At 273°K	ρ (Amagat) At 273°K	p (Atmospheres) At 273°K	ρ (Amagat) At 273°K
10.0	9.98	100.0	95.74	281.2	244.7
15.0	14.94	110.0	104.65	296.3	255.8
20.0	19.88	120.0	113.63	327.5	278.1
25.0	24.79	130.0	122.46	343.4	289.2
30.0	29.68	140.0	131.22	410.4	333.7
35.0	34.02	150.0	139.79	463.8	367.1
40.0	39.38	160.0	148.44	520.7	400.4
45.0	44.20	170.0	157.00	560.2	422.7
50.0	48.98	180.0	165.29	601.3	444.9
60.0	58.52	190.0	173.60		
70.0	67.94	200.0	181.81		
80.0	77.27	209.10	189.1		
90.0	86.50	251.6	222.5		

TABLE III (Continued)

Isothermal data for neon

P (Atmospheres) At 201°K	ρ (Amagat) At 201°K	P (Atmospheres) At 201°K	ρ (Amagat) At 201°K	P (Atmospheres) At 201°K	ρ (Amagat) At 201°K
10.0	13.54	90.0	116.87	212.8	255.8
15.0	20.27	100.0	129.07	245.7	289.2
20.0	26.97	110.0	141.12	280.4	322.6
25.0	33.63	120.0	153.08	316.8	356.0
30.0	40.26	130.0	164.82	355.0	389.3
35.0	46.85	140.0	176.34	395.2	422.7
40.0	53.39	150.0	187.76	437.8	456.1
45.0	59.90	160.0	199.04	482.3	489.4
50.0	66.38	170.0	210.12	529.3	522.8
60.0	79.23	180.0	221.08	578.9	556.2
70.0	91.92	190.0	231.83		
80.0	104.46	200.0	242.47		

experiment. Therefore, in the present experiments at low temperatures, it was assumed that no para-ortho conversion of deuterium occurred during an experiment.

CHAPTER 3

EXPERIMENTAL RESULTS AND DISCUSSION

The experimental conditions for which the enhancement absorption contours of the fundamental band of deuterium in D_2-He and D_2-Ne mixtures have been studied, are summarized in Table IV.

TABLE IV

Summary of the Experiments

Perturbing gas	Temperature (^oK)	Optical path length (cm)	Maximum density of the perturbing gas (Amagat)	Number of Experiments
Helium	273	25.8	393.0	2
"	201	25.7	504.9	3
"	77	25.7	598.0	2
Neon	298	25.8	366.6	2
"	273	25.8	399.9	2
"	201	25.7	480.2	2
"	77	25.7	416.2	2

The profiles of the pressure-induced absorption are not only dependent on the absorbing gas but also on the nature of the perturbing gas, on the temperature, and on the density. In this chapter, the profiles of the enhancement in absorption of the D_2 fundamental band in D_2-He and in D_2-Ne mixtures for different experimental conditions are presented, their shapes

are discussed, and the binary and ternary absorption coefficients are derived. Section 3.1 deals with the band in D_2-He mixtures and Section 3.2 with the band in D_2-Ne mixtures. The molecular diameters of helium and neon are derived in Section 3.3 from experimental values of the binary and ternary absorption coefficients.

3.1 Deuterium Fundamental Band in D_2-He Mixtures

(i) The Absorption Profiles:

A set of enhancement absorption profiles of the induced fundamental band of deuterium in D_2-He mixtures at each of the temperatures, 273°K, 201°K, and 77°K, is shown in Figs. 6, 7, and 8, respectively. In each of these figures, the profiles represent the enhancement in absorption of the band at several total densities of the mixture for a fixed base density of deuterium. The positions of the band origin, ν_0, and the O and S lines calculated from the constants of molecular deuterium obtained by Stoicheff (1957) from the high resolution Raman Spectrum of the low pressure gas are marked on the frequency axis. In agreement with the observations on the fundamental band of deuterium in the pure gas and in D_2-foreign gas mixtures by earlier investigators, the most striking feature of the contours in Figs. 6 to 8 is the splitting of the Q branch into two well-resolved components, Q_P and Q_R, at the low and high frequency sides of ν_0, respectively. The minima between the two components occur at ν_0 ($Q(0) = 2994\ cm^{-1}$). Recently Reddy and Lee (1968) in our laboratory studied the fundamental band of hydrogen in H_2-Ne and H_2-Kr mixtures at room temperatures and observed, in particular, certain special features in the profiles obtained in the former

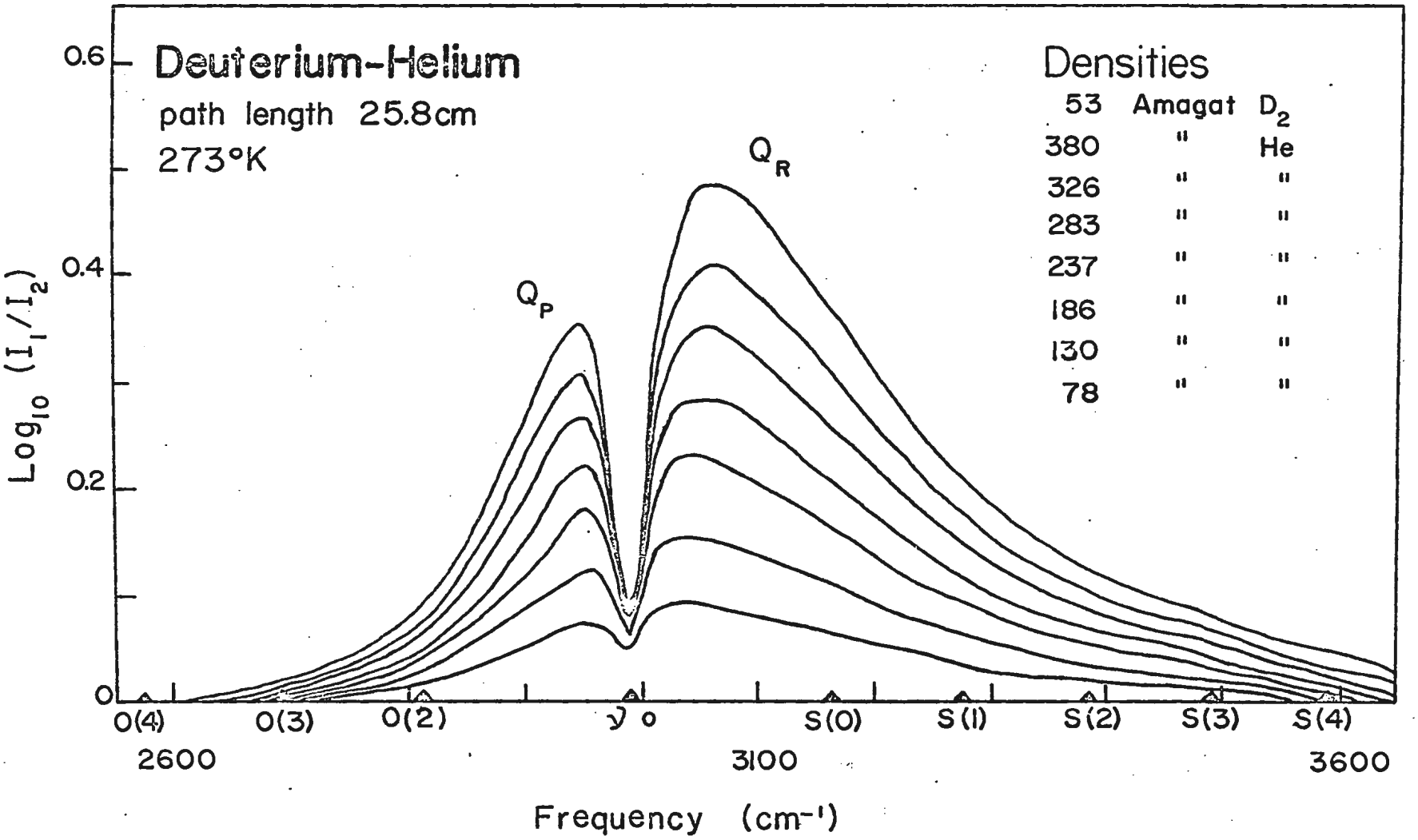

Fig. 6. The enhancement of absorption of the fundamental band of deuterium in D_2-He mixtures at 273°K.

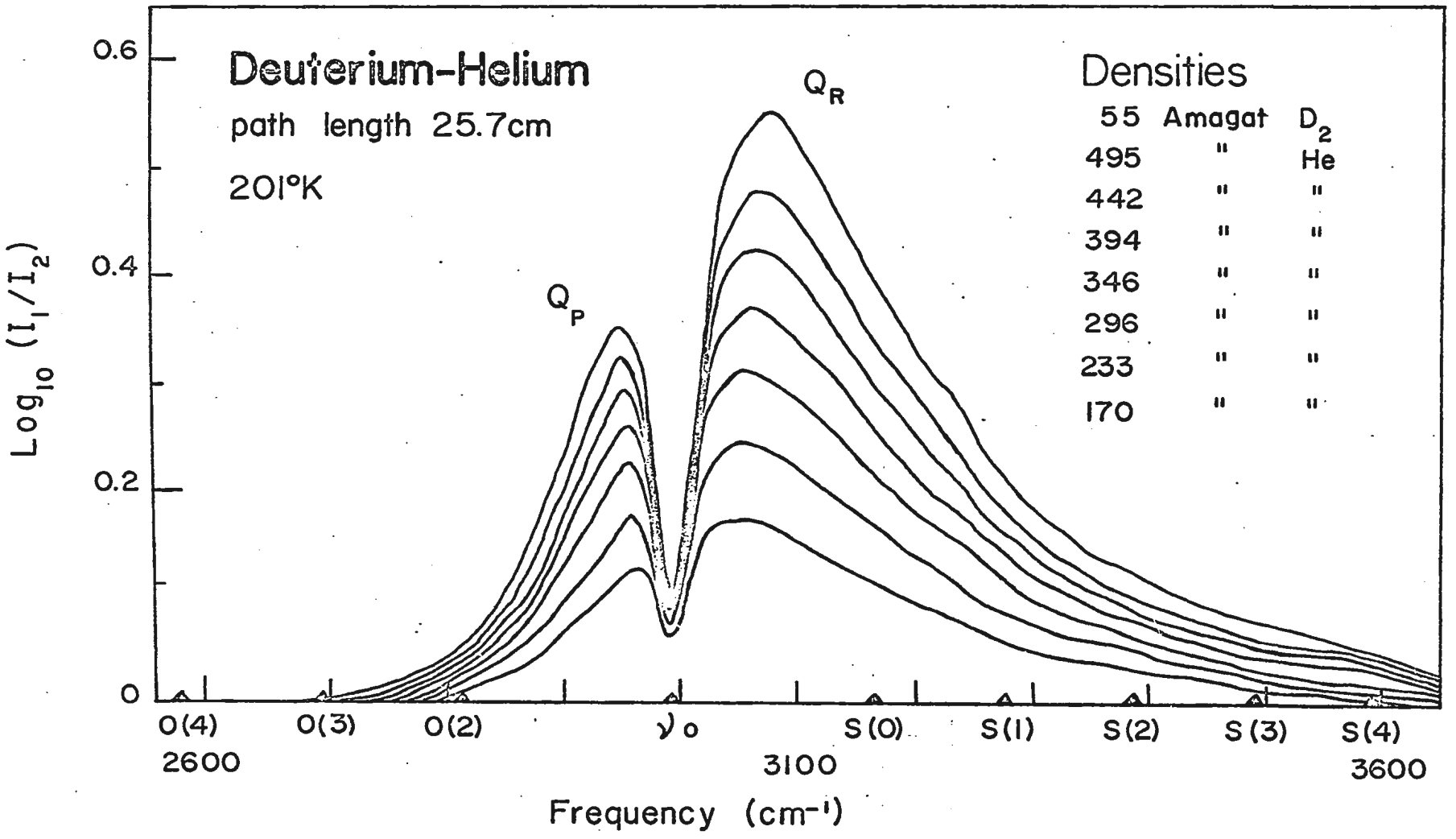

Fig. 7. The enhancement of absorption of the fundamental band of deuterium in D_2-He mixtures at 201°K.

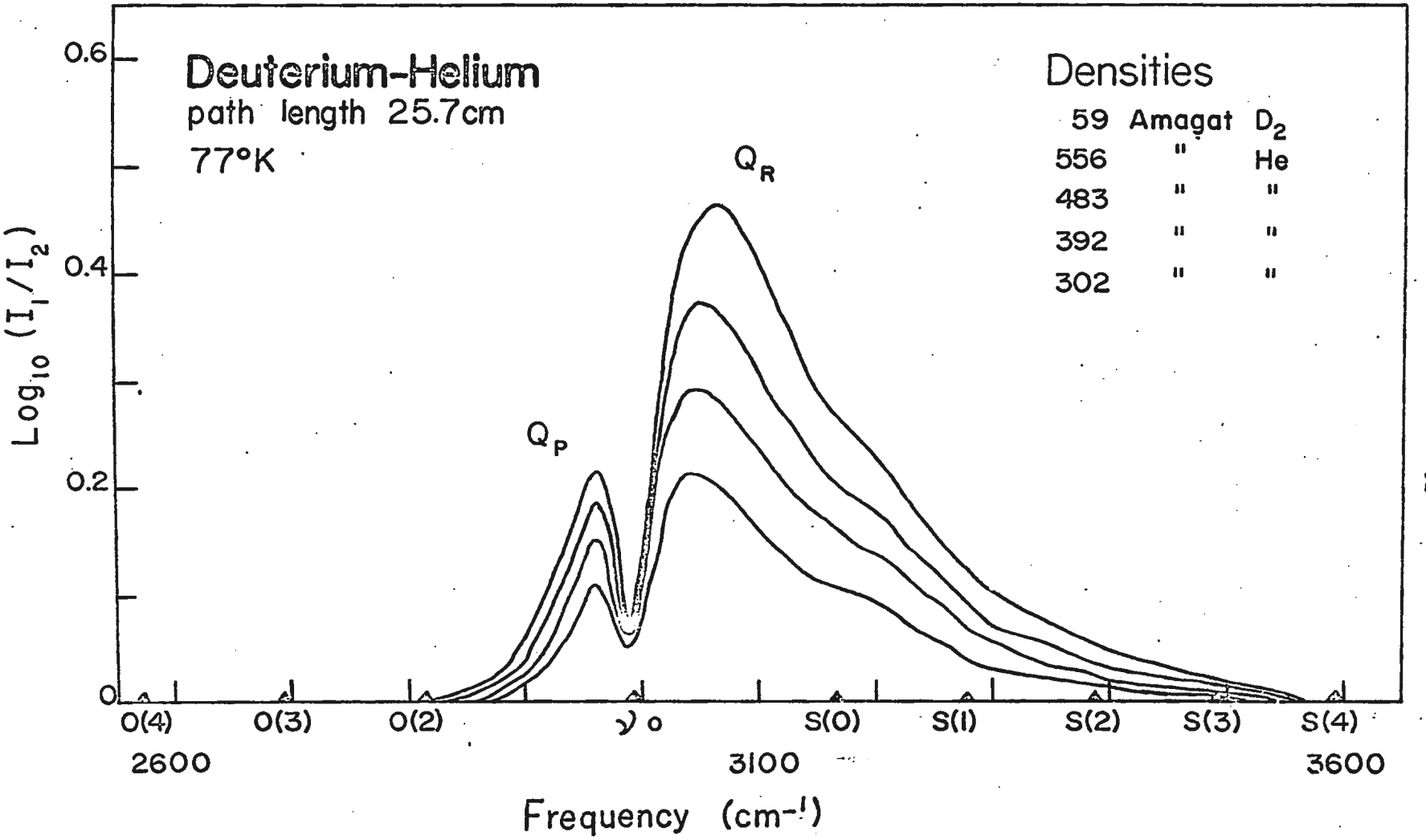

Fig. 8. The enhancement of absorption of the fundamental band of deuterium in D_2-He mixtures at 77°K.

mixtures. The splitting of the Q branch of the fundamental band of hydrogen has been explained by them in the following way: Each line Q(J) of the Q branch consists of two parts $Q_{overlap}(J)$ and $Q_{quad}(J)$ which are the contributions of the electron overlap and molecular quadrupolar interactions respectively. But the quadrupolar interaction does not contribute to the Q(0) line because the transition $J' = 0 \leftarrow J'' (= J) = 0$ is forbidden in this interaction. The components Q_R and Q_P can be interpreted as the summation and difference tones $Q_{overlap}(J) \pm \nu_K$ where ν_K is the continuum of translational frequencies in cm^{-1} that are exchanged by the absorbing molecules and the perturbing molecules during collisions. The high frequency component, Q_R, results when the absorbed photon not only changes the vibrational energy of the absorbing molecules but also increases the relative kinetic energy of the colliding molecules. The low frequency component, Q_P, results when the relative kinetic energy of the colliding system contributes to a photon which would otherwise have insufficient energy to cause the vibrational transition. The splitting of the Q branch of the fundamental band of deuterium into the Q_R and Q_P components can be explained in an exactly similar way. In all cases studied the frequency separation between the Q_P and Q_R maxima, $\Delta\nu_{PR}^{max}$ increases with the density of the perturbing gas. For the contours in Figs. 6, 7 and 8, $\Delta\nu_{PR}^{max}$ varies from 80 to 112 cm^{-1}, 82 to 128 cm^{-1} and 74 to 105 cm^{-1}, respectively. In all these enhancement contours, there is no indication of any peaks corresponding to the O and S lines. This is not unexpected since the polarizability of helium ($\alpha_{He} = 1.6\ a_0^3$, a_0 being the Bohr radius) is small (see also Chapter 4 of this thesis).

(ii) The Absorption Coefficients:

The integrated absorption coefficients of the enhancement per unit path length, $\int \alpha_{en}(\nu)d\nu$ in cm^{-1}/cm, along with the corresponding partial densities of deuterium and helium, are listed in Tables V, VI, and VII for D_2-He mixtures at 273°K, 201°K, and 77°K, respectively. In order to obtain the relation between the integrated absorption coefficients and ρ_b, the partial density of the helium gas , $\frac{1}{\rho_a \rho_b} \int \alpha_{en} d\nu$ was plotted against ρ_b for each of the D_2-He mixtures as shown in Fig. 9. The straight lines obtained indicate that the integrated absorption coefficients can be represented in the form,

$$(8) \qquad \int \alpha_{en}(\nu)d\nu = \alpha_{1b}\, \rho_a \rho_b + \alpha_{2b}\, \rho_a \rho_b^2$$

where α_{1b} and α_{2b} are the binary and ternary absorption coefficients of the enhancement, respectively. The values of α_{1b} and α_{2b} were obtained by applying a linear least square fit method and are summarized in Table VIII. Also, the modified binary absorption coefficients $\tilde{\alpha}_{1b}$ are included in this Table, as well as the values of α_{1b}, $\tilde{\alpha}_{1b}$ and α_{2b} for D_2-He at 298°K obtained by Pai, Reddy and Cho (1966). $\tilde{\alpha}_{1b}$ and the modified ternary absorption coefficient, $\tilde{\alpha}_{2b}$, are related to the integrated absorption coefficients by the equation

$$(9) \qquad c \int \tilde{\alpha}_{en}(\nu)d\nu = \tilde{\alpha}_{1b}\, \tilde{\rho}_a\, \tilde{\rho}_b + \tilde{\alpha}_{2b}\, \tilde{\rho}_a\, \tilde{\rho}_b^2$$

where $\tilde{\alpha}_{en}(\nu) = \alpha_{en}(\nu)/\nu$ is the enhancement in the absorption coefficient at a frequency ν with the frequency factor removed, $\tilde{\rho}_a$ and $\tilde{\rho}_b$ are the partial

TABLE V

Summary of Results

D_2-He mixture at ice-point temperature (273°K)

ρ_{D_2} (Amgt)	ρ_{He} (Amgt)	$\int \alpha_{en} d\nu$ (cm^{-1}/cm)
53.0	78.4	3.093
"	129.5	5.133
"	185.9	7.587
"	236.7	9.627
"	282.5	12.027
"	325.7	14.268
"	380.2	16.923
41.0	99.5	3.005
"	160.0	4.797
"	203.6	6.757
"	253.0	8.588
"	294.1	10.054
"	339.9	11.891
"	393.0	13.626

TABLE VI

Summary of Results

D_2-He mixture at alcohol-dry ice temperature (201°K)

ρ_{D_2} (Amgt)	ρ_{He} (Amgt)	$\int \alpha_{en} d\nu$ (cm^{-1}/cm)
49.9	53.9	1.357
"	119.5	3.319
"	189.9	5.482
54.9	169.9	4.993
"	233.1	7.187
"	295.8	9.352
"	345.6	11.306
"	394.2	13.018
"	441.7	14.664
"	495.4	16.792
50.1	194.9	5.666
"	249.0	7.527
"	319.6	9.841
"	372.8	11.666
"	421.7	13.376
"	504.9	16.189

TABLE VII

Summary of Results

D_2-He mixture at liquid-nitrogen temperature (77°K)

ρ_{D_2} (Amgt)	ρ_{He} (Amgt)	$\int \alpha_{end} \nu$ (cm^{-1}/cm)
71.5	175.6	3.196
"	279.0	5.642
"	351.9	7.231
"	394.5	8.278
"	457.2	9.652
"	497.5	10.796
"	557.9	12.643
"	598.0	13.800
59.6	302.9	4.304
"	392.5	6.145
"	443.5	7.198
"	483.1	7.880
"	556.4	9.950

TABLE VIII

Binary and ternary absorption coefficients for D_2-He mixtures

Temperature (^oK)	Mixture	Binary Absorption Coefficient (10^{-3} cm^{-2} Amgt^{-2})	(10^{-35}cm^{6}sec^{-1})	Ternary Absorption Coefficient (10^{-6} cm^{-2} Amgt^{-3})
298*	D_2-He	α_{1b}=0.82±0.01	$\tilde{\alpha}_{1b}$=1.08	α_{2b}=0.27±0.03
273	"	α_{1b}=0.71±0.01	$\tilde{\alpha}_{1b}$= .94	α_{2b}=+0.36±0.04
201	"	α_{1b}=0.52±0.01	$\tilde{\alpha}_{1b}$= .69	α_{2b}=+0.24±0.03
77	"	α_{1b}=0.22±0.02	$\tilde{\alpha}_{1b}$= .29	α_{2b}=+0.15±0.03

*Values quoted are from Pai, Reddy and Cho (1966)

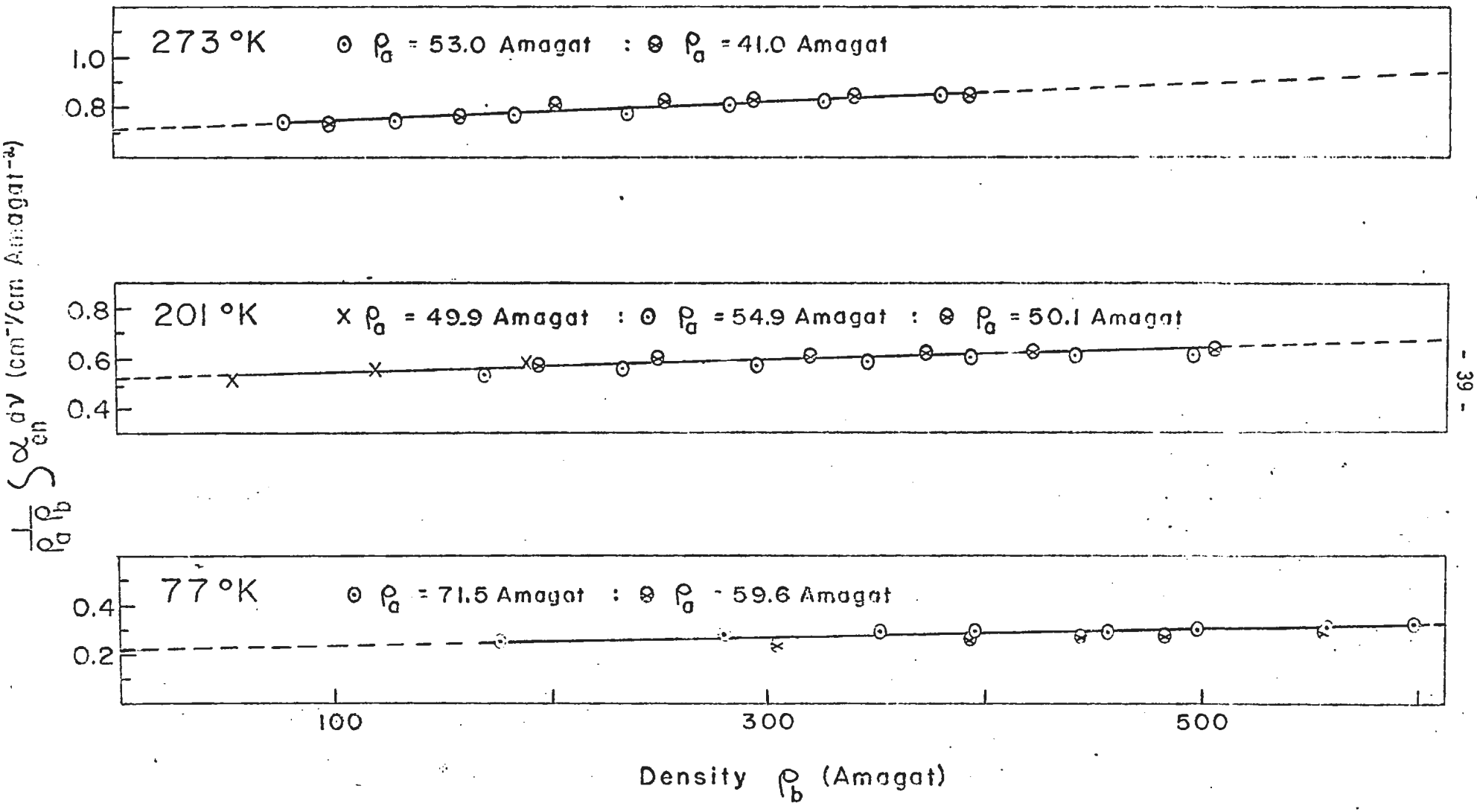

Fig. 9. The relation between the enhancements in the integrated absorption coefficients of the fundamental band of deuterium and ρ_a and ρ_b in D_2-He mixtures at 273°K, 201°K and 77°K.

number densities of the absorbing gas and the perturbing gas, respectively, and c is the speed of light. These quantities are related to α_{1b}, α_{2b}, ρ_a, and ρ_b by the following relations:

$$(10) \qquad \tilde{\alpha}_{1b} = \frac{c\,\alpha_{1b}}{\bar{\nu}} \left[\frac{V_o}{N_A}\right]^2$$

$$(11) \qquad \tilde{\alpha}_{2b} = \frac{c\,\alpha_{2b}}{\bar{\nu}} \left[\frac{V_o}{N_A}\right]^3$$

$$(12) \qquad \tilde{\rho}_a = \rho_a \frac{N_A}{V_o}$$

$$(13) \qquad \tilde{\rho}_b = \rho_\beta \frac{N_A}{V_o}$$

where V_o is the gram-molecular volume of the gas at N.T.P., N_A is Avogadro's number, and $\bar{\nu}$, which is defined by

$$(14) \qquad \bar{\nu} = \int \alpha_{en}(\nu)d\nu / \int \nu^{-1}\, \alpha_{en}(\nu)d\nu$$

is the center of the band. The values of $\bar{\nu}$ obtained for D_2-He mixtures at 273°K, 201°K, and 77°K, are 3155.8 cm^{-1}, 3141.0 cm^{-1} and 3113.8 cm^{-1}, respectively. The average value of $\bar{\nu}$ is 3136.9 cm^{-1}. The modified binary absorption coefficient, $\tilde{\alpha}_{1b}$, is independent of the frequency and represents the transition probability of absorption.

The term $\alpha_{1b}\,\rho_a\rho_b$ contained in equation (8) has been interpreted as the contribution, arising from the binary collisions between the absorbing

molecules a and the perturbing molecules b, to the enhancement absorption. The ternary term $\alpha_{2b}\,\rho_a\rho_b^2$ in equation (8) has been interpreted by previous authors (Hare and Welsh, 1958) to arise from three factors. These are (a) the finite volume effect (b) ternary collisions and (c) the change of molecular polarizability with pressure. The finite volume effect was discussed by Chisholm and Welsh (1954). At low densities, the number of absorption-inducing collisions is proportional to the product $\rho_a\rho_b$. However, when the volume of the molecules is an appreciable amount of the space which they occupy, the number of collisions increases more rapidly than the product $\rho_a\rho_b$. Secondly, ternary collisions, of the type where two molecules of the perturbing gas collide with one molecule of the absorbing gas, would annul partly the contribution of the binary collisions when a particular absorbing molecule is surrounded by a symmetrical configuration of the perturbing molecules. This so-called "cancellation effect" occurs because, in such a situation, the induced transition moment of the absorbing molecule is zero. Thirdly, it has been predicted by quantum mechanical considerations (Michels, de Boer, and Bijl 1937; de Groot and ten Seldam 1947) that there is a decrease in molecular polarizabilities at high densities. This would lower the integrated absorption coefficient to some extent, but the magnitude of the effect is difficult to estimate and is probably very small for deuterium. If we neglect this third factor, the ternary absorption coefficient α_{2b} consists essentially of two terms, a positive term due to the finite volume effect and a negative term due to the cancellation effect. The smaller value of α_{2b} for D_2-He mixtures at 77^oK than its values at higher temperatures indicates that there is more cancellation effect at 77^oK.

(iii) Discussion:

Since the ternary absorption coefficients are small compared to the binary coefficients, the binary collisions contribute most of the intensity of the induced absorption at moderate densities. In order to compare the overall absorption arising from the binary collisions between deuterium and helium molecules at different temperatures, typical experimental enhancement absorption profiles of D_2-He mixtures at 273°K, 201°K, and 77°K are presented in Fig. 10. Here the contours chosen were approximately of the same base density ρ_a and of the same density product $\rho_a\rho_b$.

It can be noticed from Fig. 10 that there is no appreciable difference between the shapes of the absorption profiles of D_2-He mixtures at 273°K, 201°K, and 77°K except for the effect of the low temperature. As the temperature of the mixture is lowered, the higher rotational levels of the absorbing molecules would be depopulated, the kinetic energy of the component gases would be decreased, and the line-widths of the individual lines would become narrower. The effect of the low temperature is seen in the profile at 77°K where the overall intensity of the band is comparatively small and the extent of the band is only from 2850 cm^{-1} to 3500 cm^{-1}. At lower temperatures the intensity of the Q_P component decreases more rapidly than that of the Q_R component. For the contours at 273°K, 201°K, and 77°K given in Fig. 10, intensity ratios $(Q_R)_{max}/(Q_P)_{max}$ are 1.37, 1.44, and 2.00 respectively.

3.2 Deuterium Fundamental Band in D_2-Ne Mixtures

(i) The Absorption Contours:

In Figs. 11, 12, 13, and 14, representative sets of enhancement

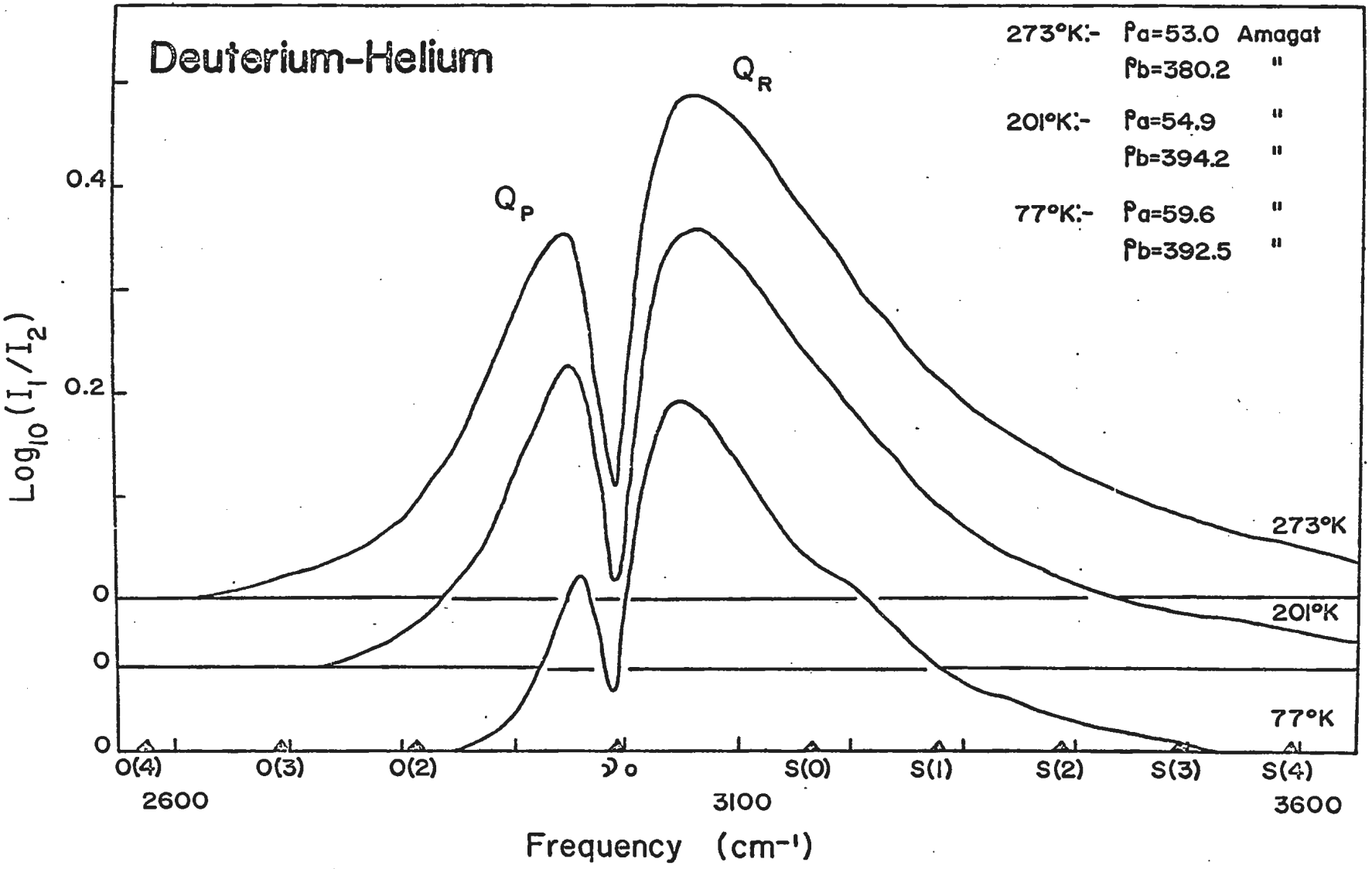

Fig. 10. Comparison of the enhancement profiles of the fundamental band of deuterium in D_2-He mixtures at 273°K, 201°K and 77°K.

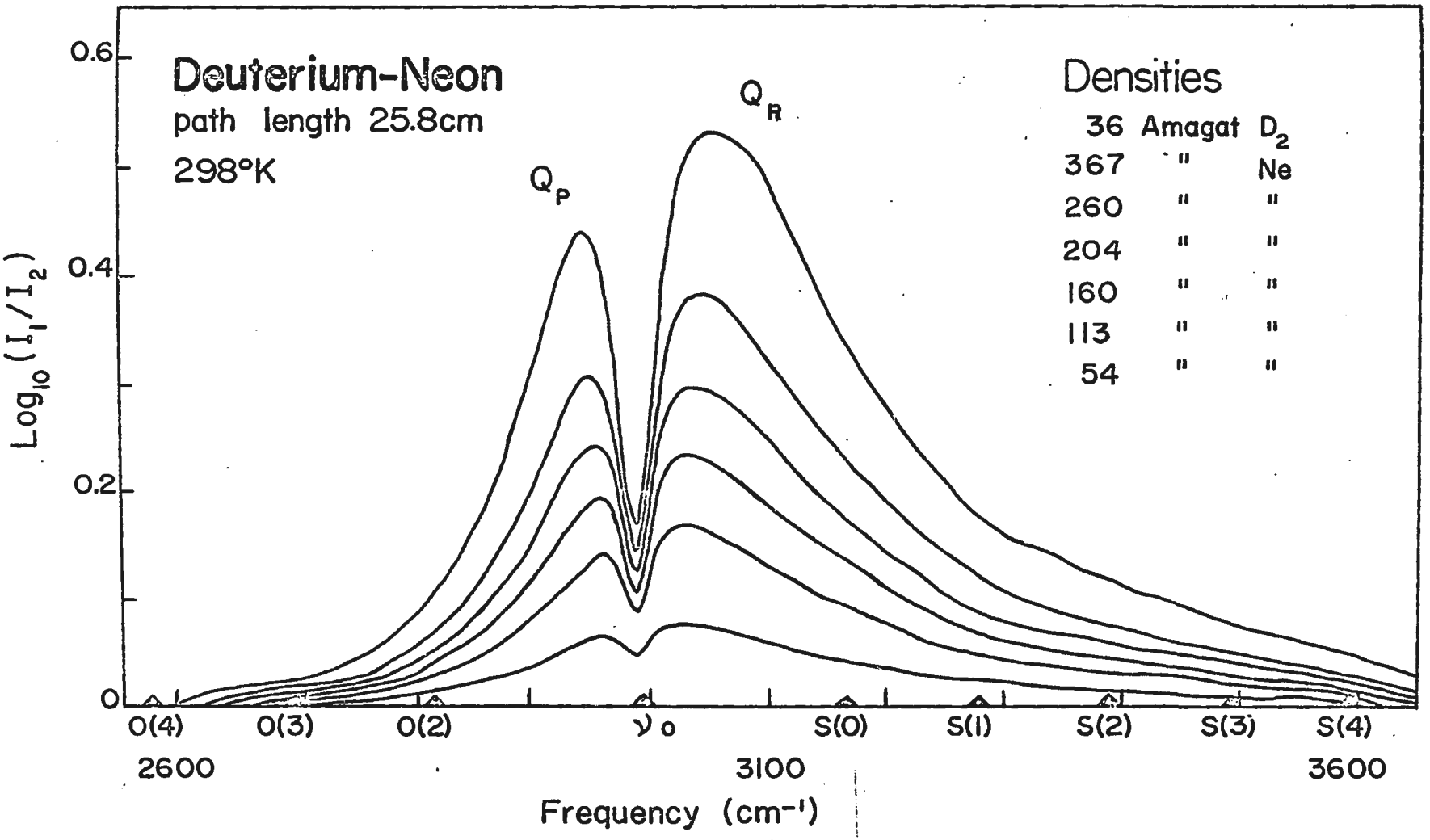

Fig. 11. The enhancement of absorption of the fundamental band of deuterium in D_2-Ne mixtures at 298°K.

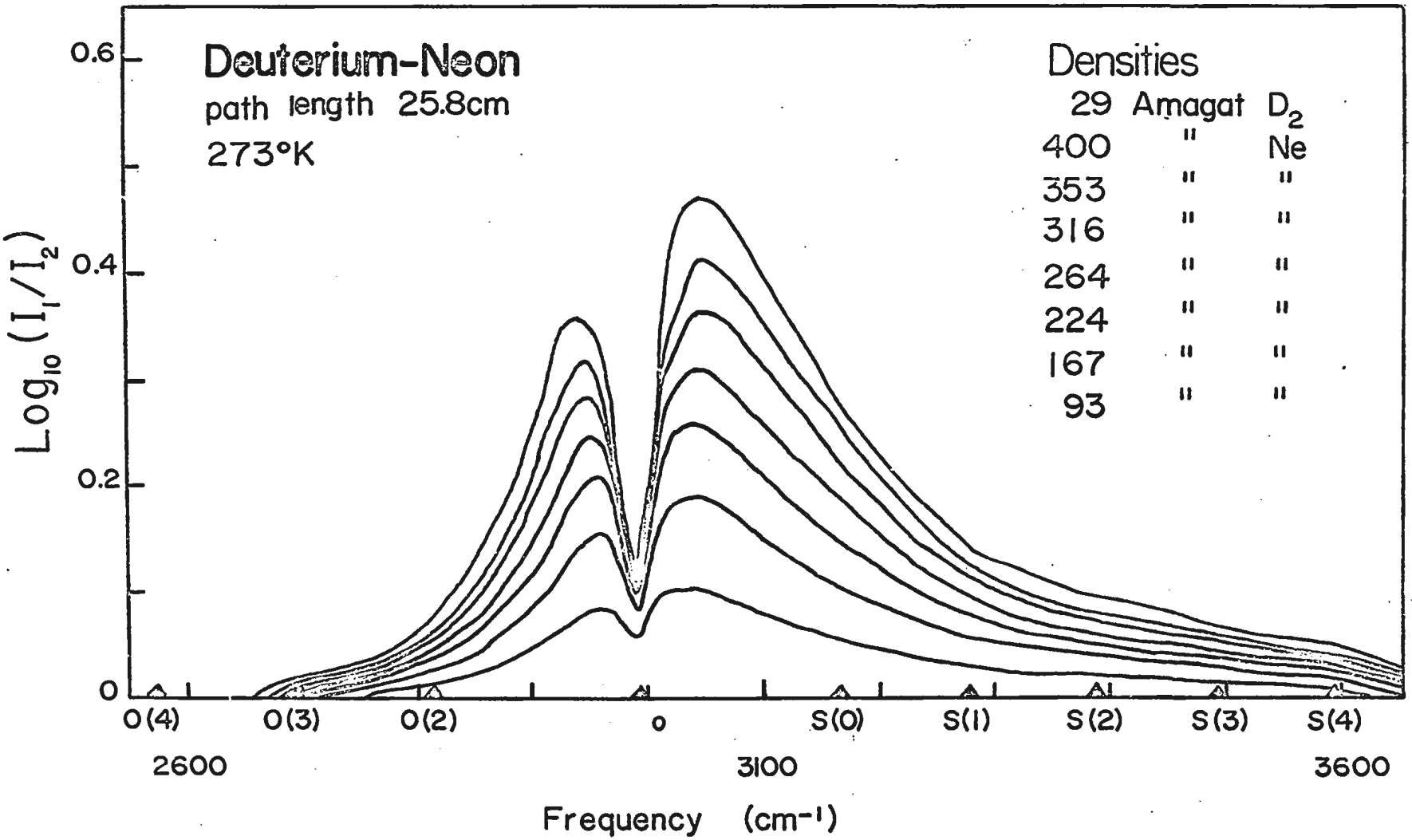

Fig. 12. The enhancement of absorption of the fundamental band of deuterium in D_2-Ne mixtures at 273°K.

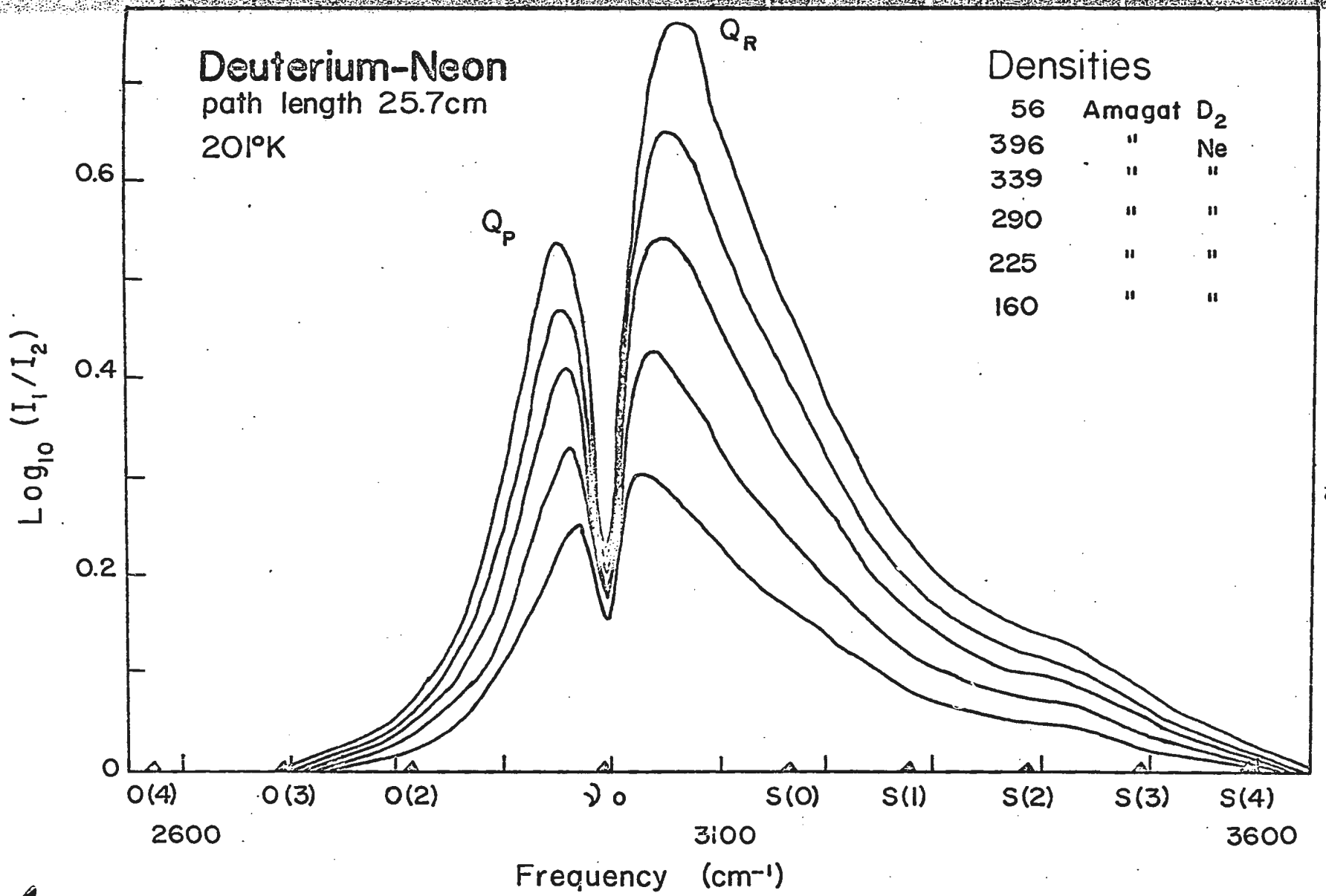

Fig. 13. The enhancement of absorption of the fundamental band of deuterium in D_2-Ne mixtures at 201°K.

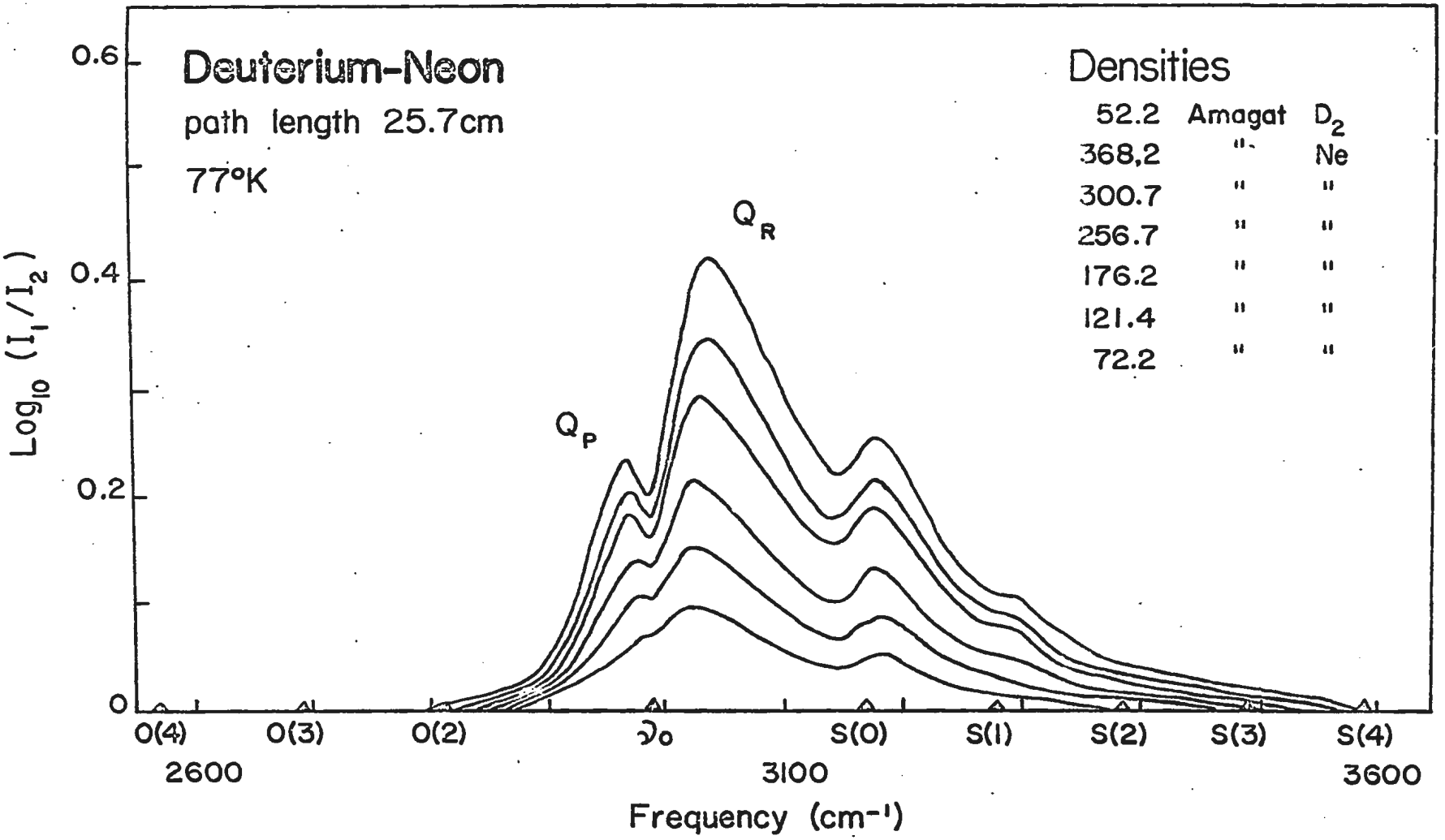

Fig. 14. The enhancement of absorption of the fundamental band of deuterium in D_2-Ne mixtures at 77°K.

absorption profiles of the induced fundamental band of deuterium in D_2-Ne mixtures at 298°K, 273°K, 201°K, and 77°K, respectively, are shown. In each figure, the profiles represent the enhancement in absorption of the band at several total densities of D_2-Ne mixtures for a fixed base density of deuterium. The splitting of the Q branch into two components, Q_P and Q_R, in D_2-Ne mixtures at 298°K, 273°K, 201°K is similar to the one in D_2-He mixtures. For the contours in Figs. 11, 12, and 13, the separation $\Delta \nu_{PR}^{max}$ varies from 60 to 108 cm^{-1}, 68 to 107 cm^{-1}, and 60 to 110 cm^{-1}, respectively. However, the profiles of the D_2-Ne mixtures at 77°K are markedly different from the others. These profiles show a well-resolved S(0) component and a S(1) component which is not as well-resolved but is distinct at higher mixture densities. For low mixture densities, there is almost no splitting of the Q branch or the appearance of the S(0) and S(1) peaks. For the D_2-Ne contours, the level of the minimum between the Q_P and Q_R components increase considerably with the density of the mixture, whereas this increase for D_2-He contours is quite small.

(ii) The Absorption Coefficients:

The principles and equations described in 3.1 (ii) for D_2-He apply also in the present case. The integrated absorption coefficients, along with the corresponding partial densities of deuterium and neon, are listed in Tables IX, X, XI, and XII for D_2-He mixtures at 298°K, 273°K, 201°K, and 77°K, respectively. In Fig. 15, the integrated absorption coefficients, $\frac{1}{\rho_a \rho_b} \int \alpha_{en} d\nu$ were plotted against ρ_b, the partial density of the neon gas, for each of the D_2-Ne mixtures. The straight lines obtained

TABLE IX

Summary of Results

D_2-Ne mixture at room temperature (298°K)

ρ_{D_2} (Amgt)	ρ_{Ne} (Amgt)	$\int \alpha_{en} d\nu$ (cm^{-1}/cm)
36.2	53.6	2.357
"	113.4	5.059
"	160.4	7.190
"	203.8	9.351
"	259.8	12.097
"	317.2	15.137
"	366.6	17.796
40.2	81.8	4.397
"	139.1	7.227
"	189.0	10.144
"	233.0	12.523
"	275.5	14.843
"	323.9	17.221
"	362.8	19.776

TABLE X

SUMMARY OF RESULTS

D_2-Ne mixture at ice-point temperature (273°K)

ρ_{D_2} (Amgt)	ρ_{He} (Amgt)	$\int \alpha_{en} d\nu$ (cm^{-1}/cm)
43.0	72.4	3.285
"	138.8	6.719
"	190.8	9.615
"	243.9	12.425
"	287.1	14.856
"	328.8	17.234
"	382.4	20.597
28.8	93.4	3.001
"	166.6	5.608
"	223.7	7.743
"	264.4	9.335
"	315.8	11.158
"	352.9	12.553
"	399.9	14.616

TABLE XI

SUMMARY OF RESULTS

D_2-Ne mixture at alcohol-dry ice temperature (201°K)

ρ_{D_2} (Amgt)	ρ_{Ne} (Amgt)	$\int \alpha_{en} d\nu$ (cm^{-1}/cm)
42.0	182.0	7.051
"	244.8	9.278
"	298.3	11.160
"	355.9	13.914
"	400.0	15.818
"	442.0	17.452
"	480.2	19.353
56.4	160.5	8.129
"	225.9	11.468
"	290.6	14.959
"	339.9	18.086
"	396.7	21.143
"	444.9	24.160

TABLE XII

Summary of Results

D_2-Ne mixture at liquid-nitrogen temperature (77°K)

ρ_{D_2} (Amgt)	ρ_{Ne} (Amgt)	$\int \alpha_{en} d\nu$ (cm^{-1}/cm)
52.2	72.2	1.798
"	121.4	3.023
"	176.2	4.449
"	256.7	6.431
"	300.7	7.514
"	342.7	8.260
"	368.2	9.164
75.1	67.0	2.355
"	107.3	3.650
"	155.3	5.162
"	250.7	8.874
"	323.5	10.971
"	416.2	14.239

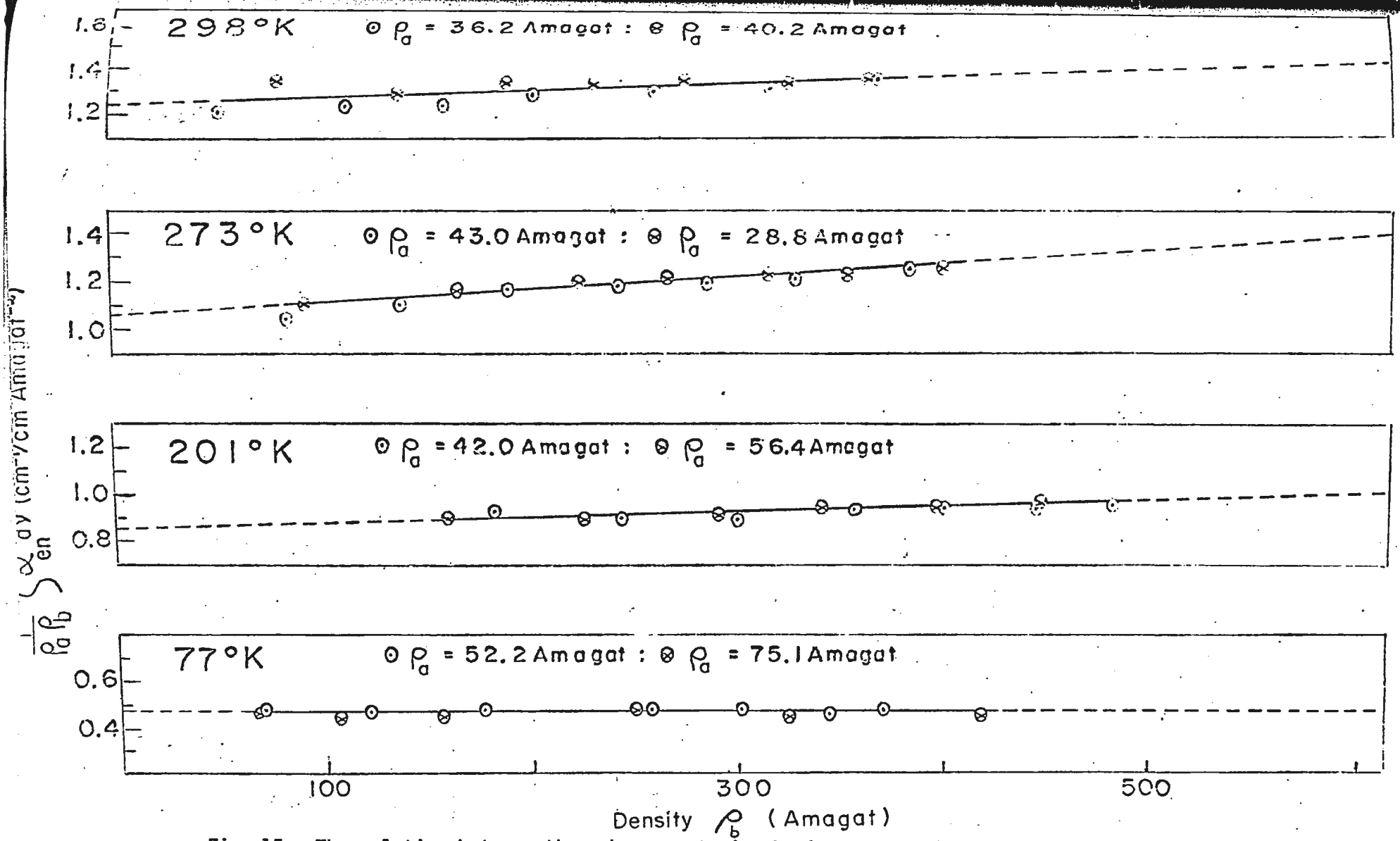

Fig. 15. The relation between the enhancements in the integrated absorption coefficients of the fundamental band of deuterium and ρ_a and ρ_b in D_2-Ne mixtures at 298°K, 273°K, 201°K and 77°K.

have positive slopes,except the one representing the D_2-Ne mixture at 77°K which has a small negative slope. This negative slope indicates the predominance of the "cancellation effect" over the other ternary collision effects, which has been explained by Hare and Welsh (1958), Van Kranendonk and Bird (1951), Van Kranendonk (1957, 1959).

The values of α_{1b} and α_{2b} obtained by applying a linear least square fit method are summarized in Table XIII for D_2-Ne at the temperatures used in these experiments. The calculated values of $\tilde{\alpha}_{1b}$ from α_{1b} are also included in the same Table. The center of the band, $\bar{\nu}$, is taken as 3092.0 cm^{-1} which is the average of the values of $\bar{\nu}$ obtained from the absorption contours of D_2-Ne mixtures at the temperatures 298°K, 273°K, 201°K, and 77°K.

(iii) Discussion:

Typical enhancement profiles of D_2-Ne mixtures at 298°K, 273°K, 201°K, and 77°K are presented collectively in Fig. 16 for the purpose of comparing the overall absorption arising from the binary collisions between deuterium and neon molecules. The basic shape of the profiles is almost the same except that of the profile at 77°K in which the components S(0) and S(1) appear distinctly. As in the case of the D_2-He profiles, the total absorption decreases, and the line widths of the individual lines become narrower, as the temperature is lowered. The intensity ratio $(Q_R)_{max}/(Q_P)_{max}$ increases as the temperature is lowered. For the contours at 298°K, 273°K, 201°K, and 77°K, these ratios are 1.20, 1.29, 1.32, and 1.58, respectively.

3.3 The Molecular Diameters of Helium and Neon

Chisholm and Welsh (1954) have estimated the effect of the finite

TABLE XIII

Binary and ternary absorption coefficients for D_2-Ne mixtures

Temperature (°K)	Mixture	Binary Absorption Coefficient (10^{-3} cm^{-2} Amgt^{-2})	(10^{-35}cm^{6}sec^{-1})	Ternary Absorption Coefficient (10^{-6} cm^{-2} Amgt^{-3})
298	D_2-Ne	α_{1b}=1.24±0.02	$\tilde{\alpha}_{1b}$=1.66	α_{2b}=+0.25±.09
273	"	α_{1b}=1.06±0.01	$\tilde{\alpha}_{1b}$=1.42	α_{2b}=+0.53±.04
201	"	α_{1b}=0.86±0.01	$\tilde{\alpha}_{1b}$=1.15	α_{2b}=+0.19±.03
77	"	α_{1b}=0.47±0.01	$\tilde{\alpha}_{1b}$= .63	α_{2b}=-0.01±.03

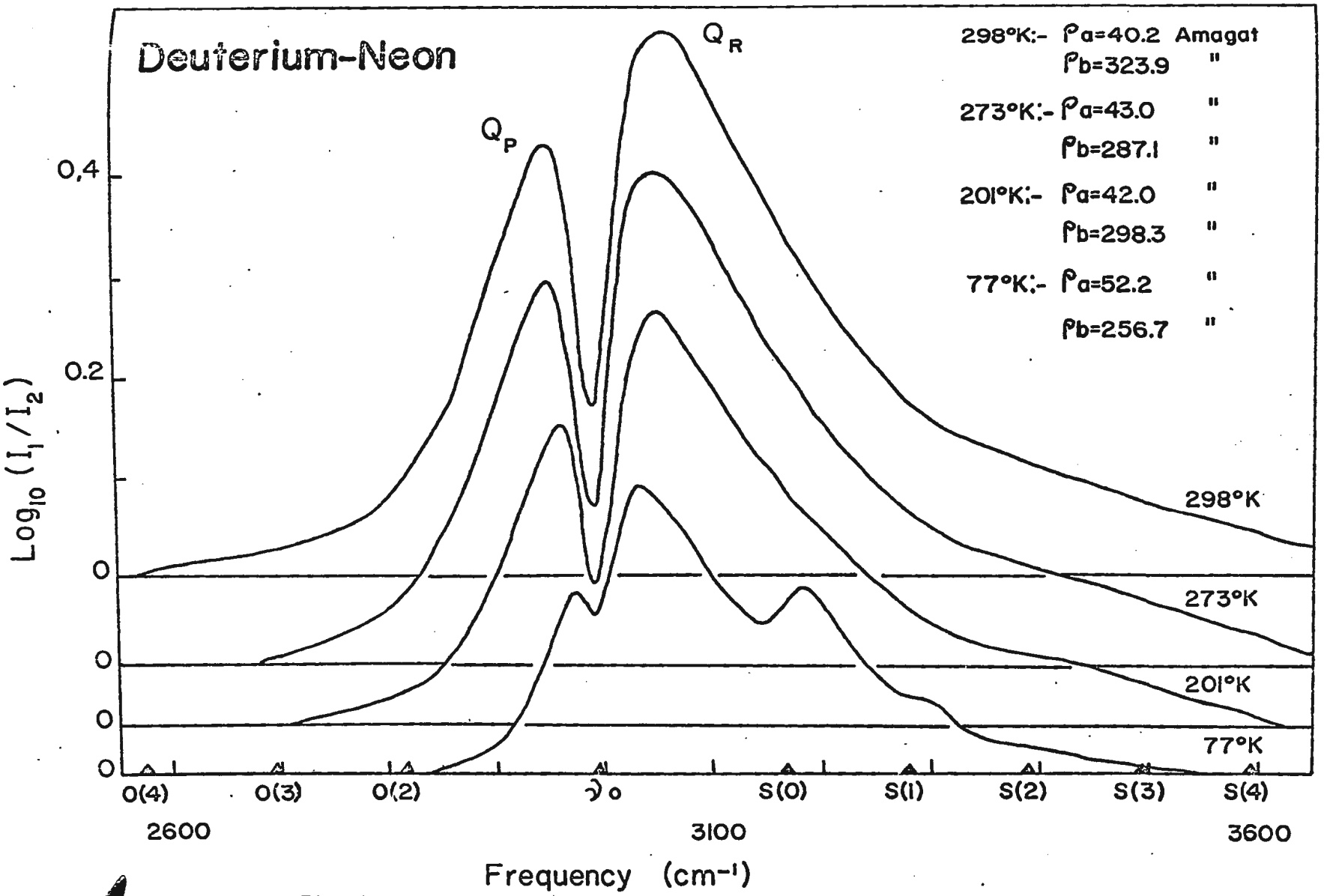

Fig. 16. Comparison of the enhancement profiles of the fundamental band of deuterium in D_2Ne mixtures at 298°K, 273°K, 201°K and 77°K.

molecular volumes on the collision frequency and consequently, on the coefficients of pressure-induced absorption. For a binary gas mixture, they have derived the following expression relating the binary and ternary absorption coefficients of the absorbing gas and the molecular diameter, D_b, of the perturbing gas:

$$(15) \qquad \alpha_{2b}/\alpha_{1b} = (4/3)\,\pi\,\frac{N}{V_o}\,D_b^{\,3}$$

where N is Avogadro's number and V_o is the molecular volume at S.T.P. Using the observed values of α_{2b} and α_{1b} for D_2-He and D_2-Ne mixtures, at 273°K representative values of the molecular diameters of helium and neon were calculated and are presented in Table XIV. Also included in Table XIV for the purpose of comparison are values of σ, which are derived from the second virial coefficient, and are taken from the summary by Hirschfelder, Curtiss and Bird (1954). The constant, σ, from the Lennard-Jones potential, is the distance of closest approach of two molecules at zero intermolecular potential. This distance corresponds to the molecules colliding with zero initial relative kinetic energy. The values of D presented in Table XIV are not very accurate because of the large errors in α_{2b} which are small quantities. The value of D for helium agrees fairly well with those of Pai (1965) and Hare and Welsh (1958). The value of D for neon is considerably smaller than σ. This was also found to be the case for the gases studied by Hare and Welsh (1958).

TABLE XIV

Molecular diameters of helium and neon

Perturbing gas	Molecular Diameter		Pai**	Hare and Welsh***
	D† (Å)	σ* (Å)	D (Å)	D (Å)
Helium	1.7	2.56	1.44	1.6
Neon	1.6	2.75	-	-

†From α_2/α_1 in the present investigation.

*The constant σ from the Lennard-Jones potential is the distance of closest approach of two molecules at zero intermolecular potential. This distance corresponds to the molecules colliding with zero initial relative kinetic energy. The values of σ are derived from the second virial coefficient and are taken from the summary by Hirschfelder, Curtiss and Bird (1954).

**Value obtained by Pai (1965).

***Value obtained by Hare and Welsh (1958).

CHAPTER 4

CALCULATIONS

4.1 Application of the Theory to the Experimental Results

According to the theory of the pressure-induced fundamental infrared absorption bands of homonuclear diatomic gases, summarized in the Appendix, the binary absorption coefficient of a mixture of a homonuclear diatomic absorbing gas with a monatomic perturbing gas can be expressed as

$$\tilde{\alpha}_{1b} = \lambda^2 \mathbf{I} \tilde{\gamma} + \left[\frac{Q_1' \alpha_2}{e \sigma^4}\right]^2 \mathbf{J} \tilde{\gamma} \qquad (16)$$

This expression is obtained from eq. (43) in the Appendix by substituting zero for the quadrupole moment of the monatomic perturbing gas, Q_2. Here Q_1' is the derivative of the quadrupole moment of the absorbing gas with respect to its internuclear distance, α_2 is the average polarizability of the perturbing gas, e is the electronic charge, σ is the Lennard-Jones intermolecular diameter, $\tilde{\gamma} = \kappa e^2 \sigma^3 = \pi e^2 \sigma^3 / 3 m_0 \nu_0$ (Appendix, eq. (29)) and λ is the dimensionless parameter (Appendix, eq. (28)). The dimensionless configurational integrals $\mathbf{I}$ and $\mathbf{J}$ are defined by equations

$$\mathbf{I} = 4\pi \int_0^\infty e^{-2(x-1)\sigma/\rho} \, g_0(x) \, x^2 dx \qquad (17)$$

and

$$\mathbf{J} = 12\pi \int_0^\infty x^{-8} \, g_0(x) \, x^2 dx \qquad (18)$$

where $x = R^* = \frac{R}{\sigma}$, R being the intermolecular separation and $g_0(x)$ is the low density limit of the pair distribution function. As outlined in the

Appendix, at higher temperatures, $g_0(x)$ is equal to $\exp(-V(x)/kT)$ classically. At intermediate temperatures, $g_0(x)$ may be expanded as an asymptotic series in powers of Planck's constant. The resulting expressions for the integrals $\mathbf{I}$ and $\mathbf{J}$ are given in the Appendix (eqs. (34) and (35)).

The term $\lambda^2 \mathbf{I}\ \tilde{\gamma}$ in eq. (16) represents the overlap part of the binary absorption coefficient whereas the other term $(Q_1' \alpha_2/e\ \sigma^4)^2 \mathbf{J}\ \tilde{\gamma}$ ($= \tilde{\alpha}^{quad}_{1b}$, say) represents the quadrupolar part. The quadrupolar part can be calculated at any temperature from the molecular constants of the component gases of the mixture and the values of $\mathbf{J}$ given by eq. (18). The calculated values of the quadrupolar parts of the deuterium fundamental band in D_2-He and D_2-Ne mixtures at the experimental temperatures are given in Table XV, together with the parameters required for the calculations. Values of the depth of the Lennard-Jones potential, ε, and those of the Lennard-Jones diameter, σ, were taken from Hirschfelder, Curtiss, and Bird (1954). For the mixtures, the geometric mean of the values of ε, and the arithmetic mean of the values of σ, of the component gases were taken. The values $\Lambda^* = (h^2/2m_{oo}\ \varepsilon\ \sigma^2)^{\frac{1}{2}}$ where m_{oo} is the reduced mass of a pair consisting of a deuterium molecule and a foreign gas molecule. The integrals, $\mathbf{J}$, at different reduced temperatures T^* ($=kT/\varepsilon$) were taken from Van Kranendonk and Kiss (1959). In calculating $\mathbf{J}$, quantum corrections $\mathbf{J}^{(2)}$ and $\mathbf{J}^{(4)}$ were applied to the classical value $\mathbf{J}_{cl}$. The values of $\tilde{\gamma}$ for the mixtures were calculated from the relation $\tilde{\gamma} = \pi e^2\sigma^3/3m_0\nu_0$ where m_0 is the reduced mass of the deuterium molecule and ν_0 is the frequency (sec^{-1}) of the

TABLE XV

Molecular constants of D_2-He and D_2-Ne mixtures and the quadrupolar parts of the binary absorption coefficients

Mixture	T (^oK)	ε/k (^oK)	σ (Å)	T*	A*	J	$\tilde{\gamma} \times 10^{32}$ ($cm^6\ sec^{-1}$)	Q_1'/ea_o (for D_2)	α_2/a_o^3 (for perturber)	$\tilde{a}^{quad}_{1b}$ ($cm^6\ sec^{-1}$)
D_2-He	298	19.44	2.742	15.33	1.805	15.59	3.290	0.56	1.4	0.06
	273	"	"	14.05	"	15.19	"	"	"	0.06
	201	"	"	10.32	"	14.01	"	"	"	0.06
	77	"	"	3.96	"	12.10	"	"	"	0.05
D_2-Ne	298	36.29	2.839	8.21	0.0988	13.34	3.652	0.56	2.7	0.16
	273	"	"	7.53	"	13.12	"	"	"	0.16
	201	"	"	5.54	"	12.51	"	"	"	0.15
	77	"	"	2.12	"	12.37	"	"	"	0.15

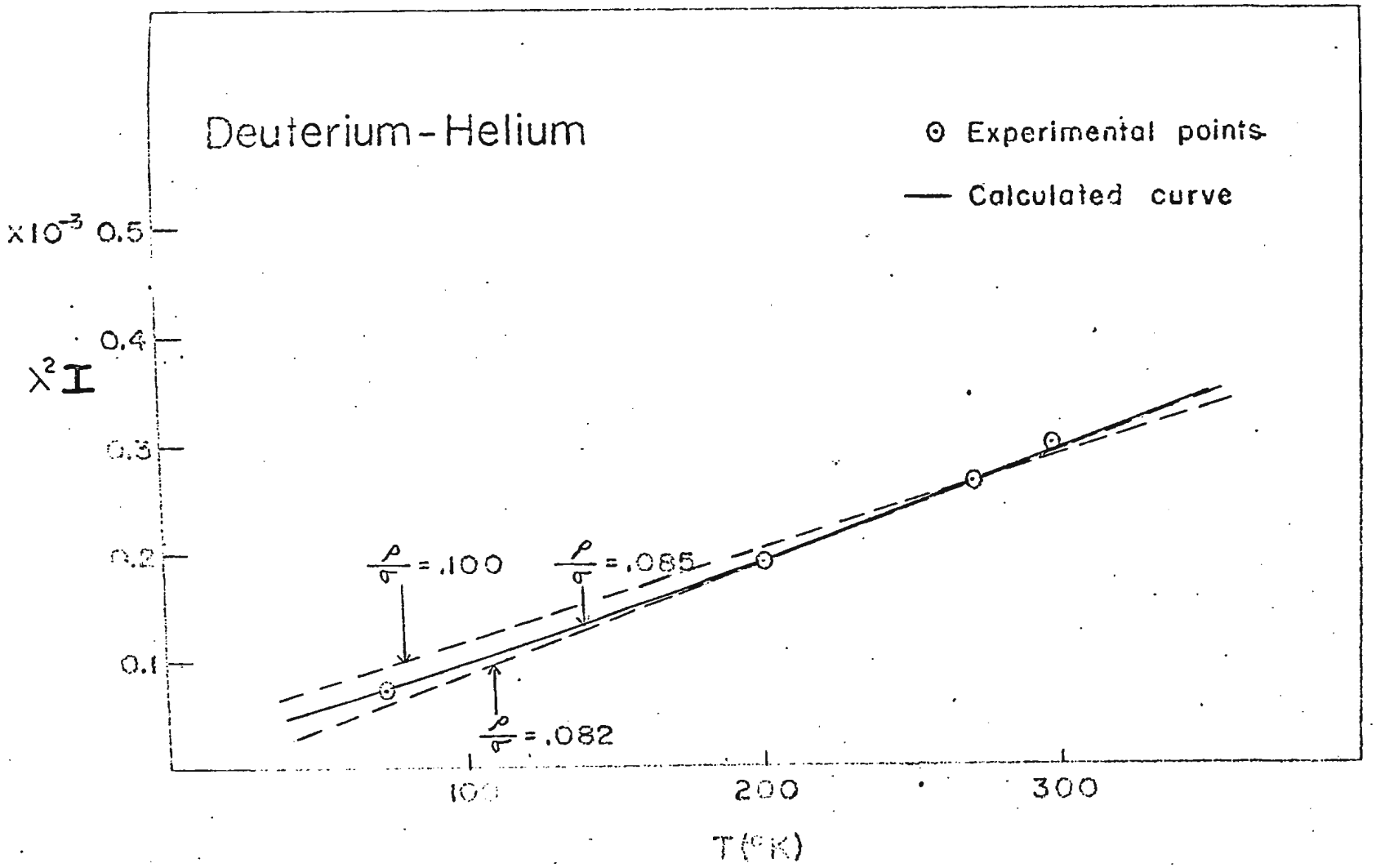

Fig. 17. Variation of $\lambda^2 I$ with the temperature for D_2-He mixtures.

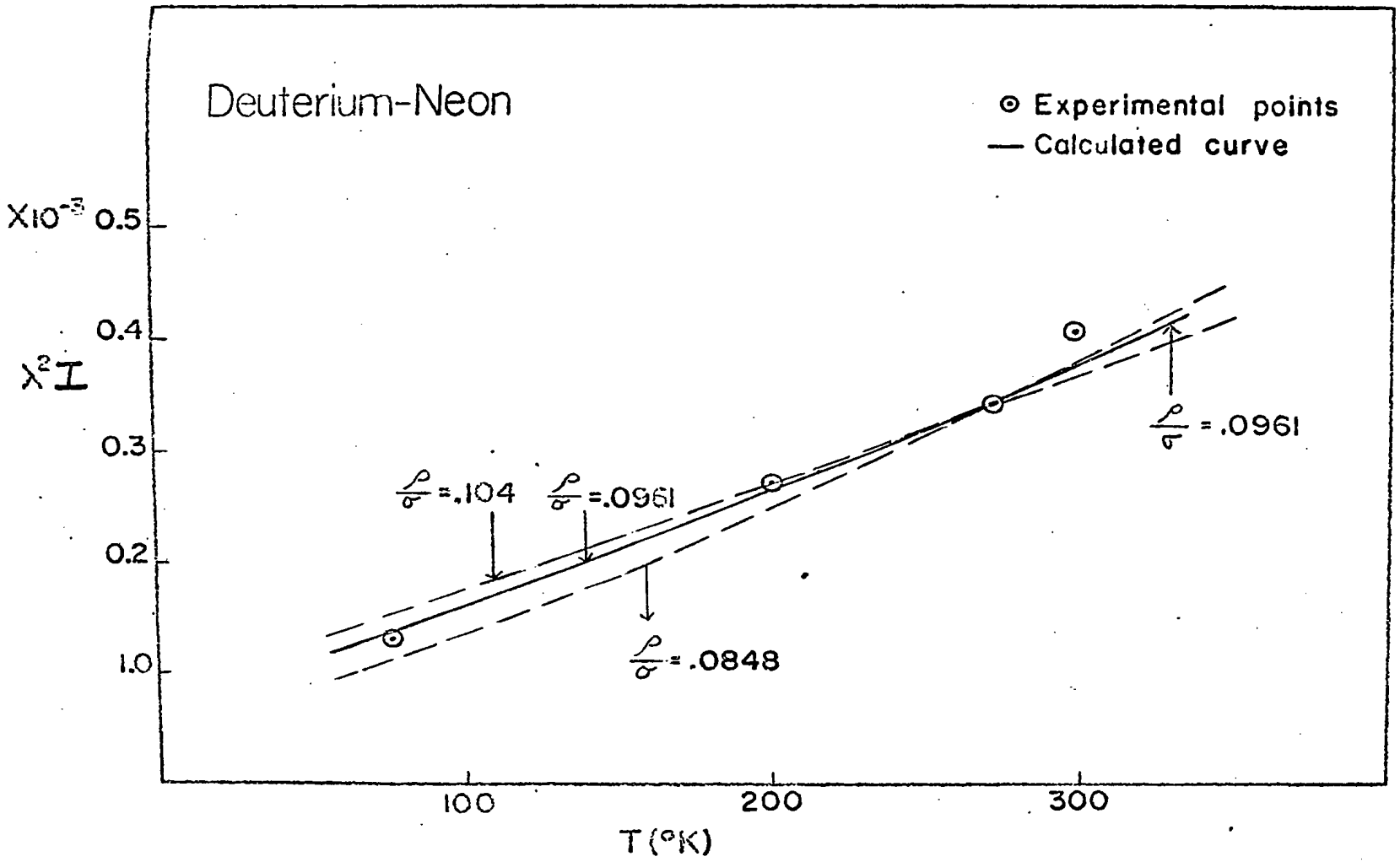

Fig. 18. Variation of $\lambda^2 I$ with the temperature for D_2-Ne mixtures.

molecular oscillation of deuterium. The derivative of the quadrupole moment, Q_1', of deuterium was assumed to be equal to that of hydrogen, and we take the theoretical value which can be derived from the calculations of Kolos and Rothaan (1960). The polarizabilities, α_2, of helium and neon were taken from Van Kranendonk (1958).

By substituting the experimental values, and the calculated values of the quadrupolar parts, of the binary absorption coefficients in eq. (16), the overlap parts $\lambda^2 I \tilde{\gamma}$ were calculated for D_2-He and D_2-Ne mixtures at different temperatures. These experimental values of the binary absorption coefficients and their quadrupolar and overlap parts are presented in Table XVI. Using the values of $\tilde{\gamma}$ given in Table XV, the values of $\lambda^2 I$ were then obtained and are given in Table XVII. These values of $\lambda^2 I$ for D_2-He and D_2-Ne mixtures were plotted against temperature $T(^oK)$ in Figs. 17 and 18 respectively. The integral I given by eq. (17) depends on the factor σ/ρ where ρ is the range of the overlap moment. One would naturally expect that the ranges ρ will be different for different mixtures. The present study of the binary absorption coefficients in D_2-He and D_2-Ne mixtures as functions of temperature enables us to determine the most probable value of σ/ρ for each of the mixtures. It may be mentioned here that the values of I were calculated for pure H_2 by Van Kranendonk and Kiss (1959) using $\rho/\sigma = 0.126$. In the present case, in order to determine the values of the ratio ρ/σ, the following procedure was adopted. The classical values of I (i.e. I_{cl}) were calculated from equation (17) using an IBM 1620 computer for twenty different ρ/σ ratios ranging from 0.082 to 0.140 at regular intervals. Quantum corrections $I^{(2)}$ and $I^{(4)}$ given by

TABLE XVI

Electron overlap and molecular quadrupole parts of the binary absorption coefficients and the parameter λ^2 of the induced fundamental band of deuterium

Mixture	Temp (^oK)	Binary Absorption Coefficients $\tilde{\alpha}_{1b} \times 10^{35}$ (cm^6 sec^{-1})	Quadrupole part $(\mu_1^2 + \mu_2^2) \mathbf{J} \tilde{\gamma} \times 10^{35}$ (cm^6 sec^{-1})	Overlap part $\lambda^2 \mathbf{I} \tilde{\gamma} \times 10^{35}$ (cm^6 sec^{-1})	Percentage (%) Quad.	Overlap
D_2-He	298*	1.08	.06	1.02	5.5	94.5
"	273	0.94	.06	0.88	6.2	93.8
"	201	0.69	.06	0.63	8.7	91.3
"	77	0.29	.05	0.24	17.2	82.8
D_2-Ne	298	1.66	.16	1.50	9.6	90.4
"	273	1.42	.16	1.26	11.3	88.7
"	201	1.15	.15	1.00	13.0	87.0
"	77	.63	.15	.48	23.8	76.2

*Values obtained by Pai, Reddy and Cho (1966)

TABLE XVII

Mixture	Temperature (°K)	$\lambda^2 I$ (cm^{-8} sec $Amgt^{-2}$)	T*	I	λ^2
D_2-He	298	3.101×10^{-4}	15.33	13.86	
"	273	2.657 "	14.05	12.54	2.11×10^5
"	201	1.915 "	10.32	8.85	
"	77	0.730 "	3.96	3.33	
D_2-Ne	298	4.107×10^{-4}	8.21	5.52	
"	273	3.450 "	7.53	5.10	6.77×10^5
"	201	2.738 "	5.54	3.92	
"	77	1.314 "	2.12	2.02	

Van Kranendonk and Kiss (1959) were then applied to I_{cl} to get the appropriate values of I. Then, for each value of ρ/σ, the value of λ^2 was calculated from $\lambda^2 I$ at 273°K using the corresponding value of I. Assuming that λ^2 is temperature-independent, the values of $\lambda^2 I$ at 298°K, 201°K and 77°K were then calculated and compared with the experimental values. This procedure was repeated until the calculated curve was found to agree closely with the experimental values. For the purpose of comparison, the experimental points of $\lambda^2 I$ and the best-fitting calculated curves, together with a few other curves for different ratios of ρ/σ are shown in Figs. 17 and 18 for D_2-He and D_2-Ne mixtures, respectively. As seen from these figures, the most probable values for ρ/σ were found to be 0.085 for D_2-He and 0.096 for D_2-Ne. The corresponding calculated values of I_{cl} are given in Table XVIII. The values of I obtained after quantum corrections were applied to I_{cl} are given in Table XVII. The values of λ^2 obtained from those of $\lambda^2 I$ and I were 2.11×10^{-5} for D_2-He and 6.77×10^{-5} for D_2-Ne.

The variation of $\tilde{\alpha}_{1b}$ with temperature for D_2-He and D_2-Ne mixtures is shown in Figs. 19 and 20, respectively. A least square fit was applied to the points and a straight line with positive slope was obtained in each case.

4.2 Variation of the Overlap and Quadrupole Parts of the Binary Absorption Coefficients

Using the values of the radial integral I corresponding to the best ratios for ρ/σ, the electron overlap parts of the binary coefficients

TABLE XVIII

Values of the radial (overlap) integral I_{cl} for ρ/σ = 0.0850 and 0.0961

Reduced Temperature (T*)	ρ/σ = 0.0850 (for D_2-He) I_{cl}	ρ/σ = 0.0961 (For D_2-Ne) I_{cl}
2.00	1.999	1.910
3.00	2.635	2.461
4.00	3.356	3.001
5.00	4.134	3.568
6.00	4.949	4.156
7.00	5.803	4.756
8.00	6.678	5.361
9.00	7.587	5.979
10.00	8.519	6.602
11.00	9.462	7.225
12.00	10.43	7.859
13.00	11.42	8.497
14.00	12.43	9.139
15.00	13.46	9.775

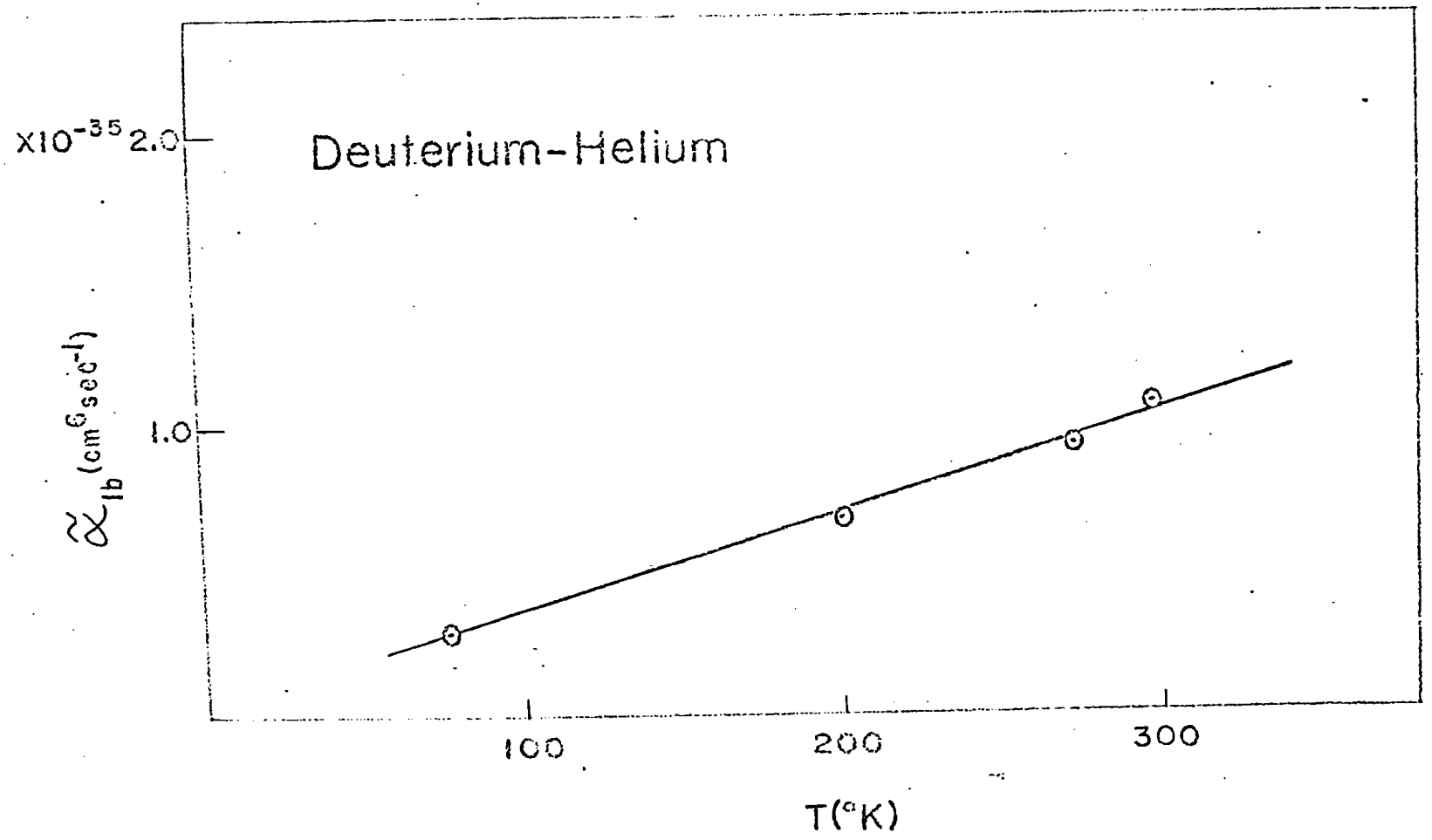

Fig. 19. Variation of $\tilde{\alpha}_{1b}$ with temperature for D_2-He mixtures.

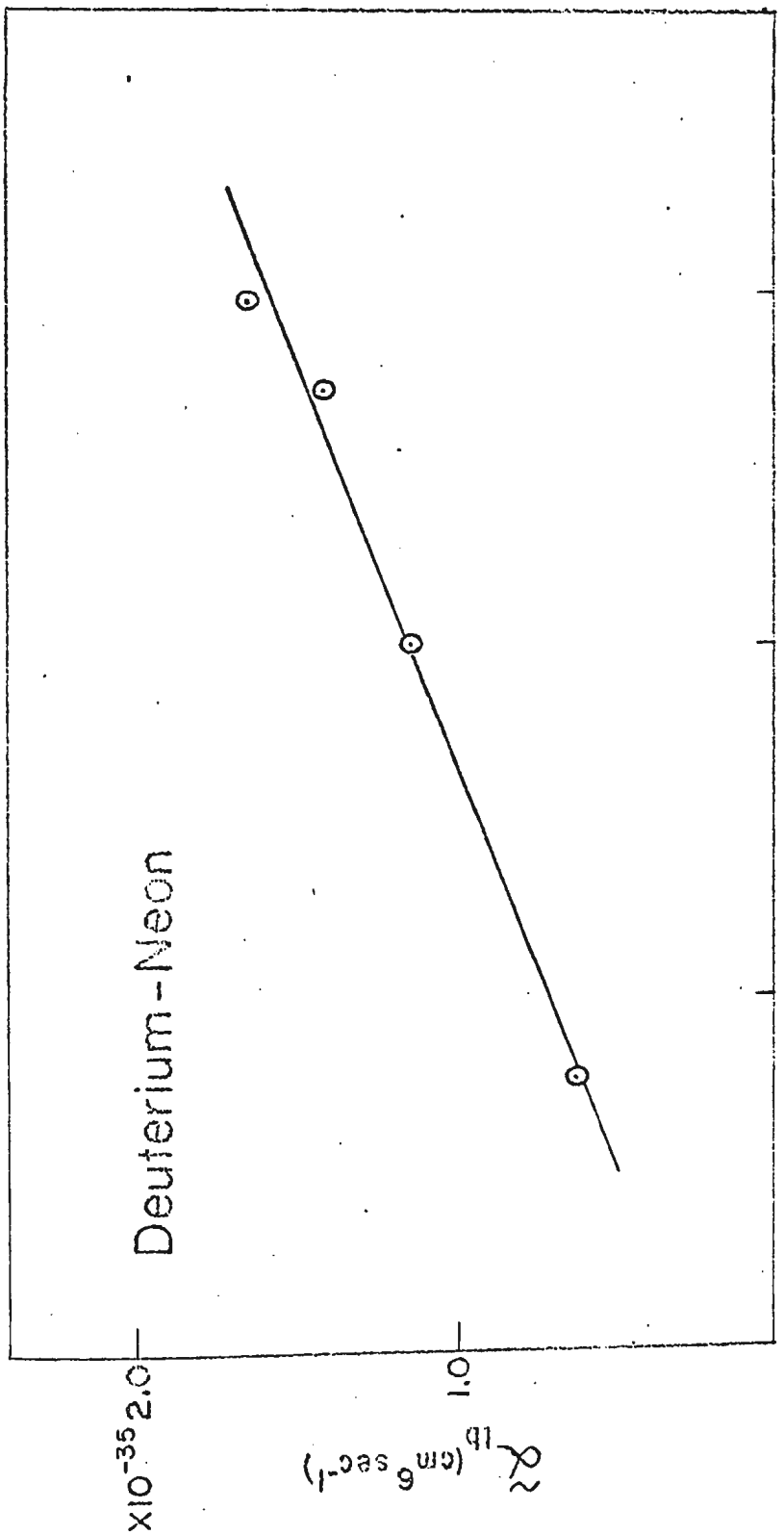

Fig. 20. Variation of $\bar{\alpha}_{1b}$ with temperature for D_2-Ne mixtures.

were calculated. The results, along with $\tilde{\alpha}_{1b}$ and the quadrupole part are summarized in Table XVI. As the quantity $\tilde{\gamma}$ for a given mixture is independent of temperature, the experimental points in Figs. 17 and 18 also represent the variation of the overlap part with temperature. Finally, using equations (24), (25), and (26) in the Appendix, the binary absorption coefficients of the individual lines of the O and S branches and the quadrupolar part (Q_{quad}) of the Q branch were calculated and the results are summarized in Table XIX.

TABLE XIX

The calculated line intensity distribution of the quadrupolar part of the binary absorption coefficients (10^{-35} cm^6 sec^{-1})

Mixture	Temperature (°K)	O(3)	O(2)	Q_{quad}	S(0)	S(1)	S(2)	S(3)	Total quadrupolar part
D_2-He	298	.005	.003	.018	.006	.015	.006	.007	.06
"	273	.004	.003	.017	.006	.015	.006	.006	.06
"	201	.003	.003	.016	.007	.017	.005	.004	.06
"	77	-	.001	.013	.015	.018	.001	-	.05
D_2-Ne	298	.009	.006	.048	.015	.040	.016	.017	.16
"	273	.009	.006	.049	.016	.042	.016	.016	.16
"	201	.006	.006	.047	.020	.047	.014	.010	.15
"	77	-	.002	.039	.048	.056	.004	-	.15

APPENDIX

THEORY OF PRESSURE-INDUCED INFRARED ABSORPTION

The pressure-induced infrared absorption spectra of homonuclear diatomic gases arise due to the dipole moments induced by intermolecular forces in clusters of two or more interacting molecules. According to the 'exp-4' model (Van Kranendonk, 1958), the dipole moment induced in a collision between a homonuclear diatomic molecule and a perturbing molecule is the sum of two parts. The first part is a short-range angle-independent electron overlap moment which occurs as a result of distortion of the electronic configuration of the colliding pair due to short-range overlap forces. This short-range moment, of strength ξ and range ρ, decreases exponentially with increasing intermolecular separation R. The second part is a long-range angle-dependent moment which results due to the polarization of one molecule by the quadrupole field of the other, and is proportional to R^{-4}. The long range moment depends on the derivatives of the quadrupole moment and the average polarizability of the absorbing molecule at the equilibrium position, $Q_1' = \left(\frac{\partial Q_1}{\partial r_1}\right)_0$ and $\alpha_1' = \left(\frac{\partial \alpha_1}{\partial r_1}\right)_0$, respectively and the quadrupole moment and the average polarizability of the perturbing molecule, Q_2 and α_2, respectively. Here r, is the internuclear distance of the absorbing molecule.

The absorption coefficient per unit path length, $\alpha(\nu)$, at a frequency $\nu(cm^{-1})$, is defined by Beer's law

(1) $$I(\nu) = I_0(\nu) \exp(-\alpha(\nu)\ell)$$

where $I_0(\nu)$ is the intensity incident on an evacuated absorption cell of

length ℓ, and $I(\nu)$ is the intensity transmitted by the cell containing the absorbing (pure) gas. The enhancement in the absorption coefficient per unit path length, $\alpha_{en}(\nu)$ at a frequency ν due to the addition of a foreign gas to the cell containing the absorbing gas at a particular base density is given by

$$I_2(\nu) = I_1(\nu) \exp(-\alpha_{en}(\nu)\ell) \tag{2}$$

where $I_1(\nu)$ is the intensity transmitted by the absorbing gas in the cell, and $I_2(\nu)$ is the intensity with the binary mixture in the cell. Eqs. (1) and (2) can be simplified as

$$\alpha(\nu) = \frac{2.203}{\ell} \log_{10} \frac{I_0}{I} \tag{3}$$

and

$$\alpha_{en}(\nu) = \frac{2.303}{\ell} \log_{10} \frac{I_1}{I_2} \tag{4}$$

The integrated absorption coefficient for the pressure-induced fundamental bands of homonuclear diatomic gases can be generally expressed in terms of the powers of the densities of the gases in Amagat units. For a pure gas at a density ρ_a, the integrated absorption coefficient can be expressed in the form

$$\int \alpha(\nu) d\nu = \alpha_{1a} \rho_a^2 + \alpha_{2a} \rho_a^3 + \text{-----} \tag{5}$$

For a binary gas mixture, the enhancement of the integrated absorption coefficient due to the addition of a foreign gas with a partial density ρ_b to the pure gas in the absorption cell at a density ρ_a is given by

(6) $$\int \alpha_{en}(\nu)d\nu = \alpha_{1b}\rho_a\rho_b + \alpha_{2b}\rho_a\rho_b^2 + \text{--------}$$

Here α_{1a} or α_{1b}(cm^{-2} $Amagat^{-2}$) is the binary absorption coefficient and α_{2a} or α_{2b}(cm^{-2} $Amagat^{-3}$) is the ternary absorption coefficient. The absorption coefficient $\alpha(\nu)$ or $\alpha_{en}(\nu)$ at any frequency ν is dependent directly on ν itself. The integrated absorption in eq. (5) or (6) is proportional to the absorbed energy. To obtain the transition probability for the pressure-induced vibration bands, the absorption coefficients $\alpha(\nu)$and $\alpha_{en}(\nu)$ in eqs. (5) and (6) must be replaced by $\alpha(\nu)/\nu$ and $\alpha_{en}(\nu)/\nu$ respectively. When this is done, the binary and ternary absorption coefficients can be converted into new forms so that they are more directly related to the transition probabilities due to the binary and ternary collisions respectively. The corresponding expressions are

(7) $$\tilde{\alpha}_{1a} = \frac{c\alpha_{1a}}{\bar{\nu}}\left[\frac{V_o}{N_A}\right]^2 ; \quad \tilde{\alpha}_{2a} = \frac{c\alpha_{2a}}{\bar{\nu}}\left[\frac{V_o}{N_A}\right]^3$$

and

(8) $$\tilde{\alpha}_{1b} = \frac{c\alpha_{1b}}{\bar{\nu}}\left[\frac{V_o}{N_A}\right]^2 ; \quad \tilde{\alpha}_{2b} = \frac{c\alpha_{2b}}{\bar{\nu}}\left[\frac{V_o}{N_A}\right]^3$$

Here

(9) $$\bar{\nu} = \int\alpha(\nu)d\nu / \int\alpha(\nu)\nu^{-1}\,d\nu$$

is the band centre, V_o is the gram molecular volume at S.T.P., N_A is the Avogadro number, c is the speed of light and ν is the frequency in wave-numbers. The integrated absorption coefficients can now be written as

(10) $$c\int\tilde{\alpha}(\nu)d\nu = \tilde{\alpha}_{1a}\tilde{\rho}_a^2 + \tilde{\alpha}_{2a}\tilde{\rho}_a^3 + \text{-----}$$

and

$$(11) \qquad c \int \tilde{\alpha}_{en}(\nu) d\nu = \tilde{\alpha}_{1b} \tilde{\rho}_a \tilde{\rho}_b + \tilde{\alpha}_{2b} \tilde{\rho}_a \tilde{\rho}_b^2 + \text{-----}$$

where $\tilde{\alpha}(\nu) = \alpha(\nu)/\nu$ is an absorption coefficient independent of frequency, and $\tilde{\rho}_a$ $(=\rho_a \frac{N_A}{V_o})$ and $\tilde{\rho}_b$ $(=\rho_b \frac{N_A}{V_o})$ are number densities of the absorbing gas "a" and the perturbing gas "b" respectively in a given mixture.

According to Van Kranendonk (1957), the binary absorption coefficient of a definite rotational branch B of the fundamental band of a pure homonuclear diatomic gas is given by

$$(12) \qquad \tilde{\alpha}_{1a}(B) = \kappa \Sigma^{(B)} P_1 P_2 \int |M(\omega_1, \omega_2, R_{12})|^2 g_0(R_{12}) dR_{12}$$

where the suffixes 1 and 2 represent the colliding molecules, $K = \pi/3\, m_0 \nu_0$, m_0 being the reduced mass of the absorbing molecule, ν_0 is the frequency of molecular oscillation or the band origin (expressed in sec^{-1}), P_1 and P_2 are the normalized Boltzmann factors for the initial states of molecules 1 and 2, normalized in such a way that

$$(13) \qquad \sum_J (2J + 1) P(J) = 1,$$

R_{12} is the positive vector joining the centres of mass of the two molecules, and $g_0(R_{12})$ is the pair distribution function arising from the pair of molecules (1, 2). Van Kranendonk (1958) represented the induced dipole moment M by the expression,

$$(14) \qquad M(\omega_1, \omega_2, R_{12}) = 4\pi \sum_{\lambda_1 \mu_1 \lambda_2 \mu_2} D(\lambda_1 \mu_1, \lambda_2 \mu_2 R_{12}) Y_{\lambda_1}^{\mu_1}(\omega_1) Y_{\lambda_2}^{\mu_2}(\omega_2)$$

where $\omega_1 = (\theta_1, \phi_1)$ and $\omega_2 = (\theta_2, \phi_2)$ specify the polar angles of the inter-nuclear axes of the molecules 1 and 2 relative to a coordinate frame xyz the z-axis of which lies along the vector R_{12} that connects the centre of mass of molecule 1 to that of molecule 2, and μ_1 and μ_2 are the projection quantum numbers of the angular moment λ_1 and λ_2 along an axis perpendicular to R_{12}. The components D_μ of the expansion coefficient D in the same coordinate frame are characteristic of the pair of colliding molecules. $\mu = 1, 0, -1$ refers to the components

$$(15) \qquad D_{\pm 1} = \frac{1}{\sqrt{2}} (D_x \pm i D_y) \; ; \; D_0 = D_z \; .$$

For the homonuclear diatomic molecules the centre of mass coincides with the centre of symmetry of the charge distribution, and D_μ are different from zero only for even values of λ_1 and λ_2. However, when the centre of mass does not coincide with the centre of symmetry of the charge distribution, D_μ are different from zero also for odd values of λ_1 and λ_2. The components D_μ are assumed to have the following values:

$$(16) \qquad D_0 (00, 00) = \xi \exp (-R/\rho) \; ,$$

$$(17) \qquad D_0 (20, 00) = \frac{3}{\sqrt{5}} \frac{Q_1' \alpha_2}{R^4} \; ,$$

$$(18) \qquad D_0 (00, 20) = \frac{3}{\sqrt{5}} \frac{\alpha_1' Q_2}{R^4} \; ,$$

$$(19) \qquad D_{\pm 1} (2\pm 1, 00) = + \frac{3}{\sqrt{15}} \frac{Q_1' \alpha_2}{R^4} \; ,$$

$$(20) \qquad D_{\pm 1} (00, 2\pm 1) = - \frac{3}{\sqrt{15}} \frac{\alpha_1' Q_2}{R^4} \; .$$

The functions $Y_{\lambda}^{\mu}(\omega)$ in equation (16) are spherical harmonics which can be expressed as

(20a) $$Y_{\lambda}^{\mu}(\omega) = \left((2\lambda+1)\,(\lambda-|\mu|)!/4\pi(\lambda+|\mu|)! \right)^{\frac{1}{2}} P_{\lambda}^{\mu}(\cos\theta) e^{j\mu\phi}$$ and

are dimensionless. Hence, the coefficients D_{μ} have the dimensions of dipole moment. The first coefficient $D_0(00,00)$ which decreases exponentially with the increasing intermolecular distance R can be considered as the dipole moment induced by the short-range overlap forces, while the other coefficients in equations (17) to (20) can be considered as the contributions of the long-range forces to the induced dipole moment.

The binary absorption coefficients of the individual lines, with the rotational quantum number J (selection rule $\Delta J = 0, \pm 2$), of the O, Q and S branches of the induced fundamental band are expressed as follows:

For the pure gas

(21) $$\tilde{\alpha}_{1a}(O(J)) = (\mu_1^2 + \mu_2^2)\, \mathbf{J}\, \tilde{\gamma}\, P(J)\, L_2(J, J-2)\,,$$

(22) $$\tilde{\alpha}_{1a}(Q(J)) = \lambda^2\, \mathbf{I}\, \tilde{\gamma}\, P(J) L_0(J, J) + \mu_1^2\, \mathbf{J}\, \tilde{\gamma}\, P(J)\, L_2(J,J) + \mu_2^2\, \mathbf{J}\, \tilde{\gamma}\, P(J) L_0(J,J) \sum_{J'} P(J') L_2(J',J'),$$

and

(23) $$\tilde{\alpha}_{1a}(S(J)) = (\mu_1^2 + \mu_2^2)\, \mathbf{J}\, \tilde{\gamma}\, P(J)\, L_2(J, J+2).$$

For the mixtures

(24) $$\tilde{\alpha}_{1b}(O(J)) = (\mu_1^2 + \mu_2^2)\, \mathbf{J}\, \tilde{\gamma}\, P(J)\, L_2(J, J-2),$$

$$(25)\qquad \tilde{\alpha}_{1b}\,(Q(J)) = \lambda^2 \mathbf{I}\,\tilde{\gamma}\,P(J)L_0(J,J) + \mu_1^{\,2}\,\mathbf{J}\,\tilde{\gamma}P(J)L_2(J,J) + \mu_2^{\,2}\,\mathbf{J}\,\tilde{\gamma}\,P(J)L_0(J,J),$$

and

$$(26)\qquad \tilde{\alpha}_{1b}\,(S(J)) = (\mu_1^{\,2} + \mu_2^{\,2})\,\mathbf{J}\,\tilde{\gamma}\,P(J)L_2(J,J+2).$$

Here, the parameters μ_1, μ_2, and λ are dimensionless and are defined by

$$(27)\qquad \mu_1 = \frac{Q_1'\alpha_2}{e\sigma^4}\;;\;\mu_2 = \frac{\alpha_1' Q_2}{e\sigma^4}$$

$$(28)\qquad \lambda = \frac{\xi}{e}\quad \exp\,(-\sigma/\rho)$$

where σ is the intermolecular distance R for which the intermolecular potential V(R) is zero, and e is the absolute value of the electronic charge. The parameter λ is significant in that λe represents the amplitude of the oscillating overlap dipole moment when the molecules are a distance σ apart. Similarly, μ_1 e and μ_2e represent the amplitudes of the quadrupole moment. $\tilde{\gamma}$ is defined by

$$(29)\qquad \tilde{\gamma} = \frac{\pi\, e^2\sigma^3}{3\, m_0 v_0}\quad .$$

$\mathbf{I}$ and $\mathbf{J}$ are radial distribution integrals and are defined by

$$(30)\qquad \mathbf{I} = 4\pi \int_0^\infty \exp\,(-2(x-1)\sigma/\rho)\; g_0\,(x)\; x^2 d\,x$$

and

$$(31)\qquad \mathbf{J} = 12\pi \int_0^\infty x^{-8}\; g_0(x)\; x^2 d\,x$$

where $x = R/\sigma$ and $g_0(x)$ is the low density limit of the pair distribution function. At higher temperatures the classical values (I_{cl} and J_{cl}) of I and J can be calculated using the pair distribution function.

(32) $$g_0(x) = \exp(-V(x)/kT).$$

Here $V(x)$ is taken as the Lennard-Jones intermolecular potential which is expressed as

(33) $$V(x) = 4\varepsilon (x^{-12} - x^{-6})$$

where ε is the depth of the potential. At intermediate temperatures, the pair distribution function $g_0(x)$ can be expanded as an asymptotic series in powers of the Planck's constant, h. The resulting expansions of the quantities I and J are given by Van Kranendonk and Kiss (1959)

(34) $$I = I_{cl} - \Lambda^{*2} I^{(2)} + \Lambda^{*4} I^{(4)}$$

and

(35) $$J = J_{cl} - \Lambda^{*2} J^{(2)} + \Lambda^{*4} J^{(4)}$$

where

(36) $$\Lambda^* = (h^2/ 2 m_{00} \varepsilon \sigma^2)^{\frac{1}{2}}$$

is the reduced mean de Broglie wavelength, m_{00} being the reduced mass of the colliding pair of molecules. At lower temperatures, the pair distribution function must be calculated entirely quantum mechanically from the radial wave function of the two molecules. This has been done for hydrogen by Poll (1960). The quantities $L_\lambda(J,J')$ in equations (21) to (26) are Racah

coefficients which satisfy the relation

$$(37) \qquad \sum_{J'} L_{\lambda} (J, J') = 2J + 1,$$

and are given by

$$(38) \qquad L_0 (J, J) = 2J + 1$$

$$(39) \qquad L_2 (J, J-2) = 3 (J-1) J/2(2J-1)$$

$$(40) \qquad L_2 (J, J+2) = 3 (J+1) (J+2)/2 (2J+3)$$

and

$$(41) \qquad L_2 (J, J) = J (J+1) (2J+1)/ (2J - 1) (2J + 3).$$

The normalized Boltzmann factors P(J) of a homonuclear diatomic gas in various rotational states J of the ground vibrational level (v = 0), occurring in equations (21) to (26), is given by

$$(42) \qquad P(J) = \frac{g_n \exp [- B_0 J (J+1) hc/kT]}{\sum_{J} (2J+1) g_n \exp [-B_0 J(J+1) hc/kT]}$$

where g_n (= 2T+1) is the nuclear spin degeneracy, T being the total nuclear spin of the molecule, B_0 is the rotational constant for the ground vibrational level. When the perturbing molecules, b, are monatomic, Q_2 equals zero, and hence μ_2 equals zero. The total binary absorption coefficients, $\tilde{\alpha}_{1a}$ and $\tilde{\alpha}_{1b}$, for the fundamental band are obtained by adding, after summing over J, equations (21), (22) and (23) for the pure gas and equations (24), (25) and (26) for a binary mixture. The resulting single expression for both cases

can be written as

$$(43) \qquad \tilde{\alpha}_{1a} \text{ or } \tilde{\alpha}_{1b} = \lambda^2 \mathbf{I}\, \tilde{\gamma} + (\mu_1^2 + \mu_2^2)\, \mathbf{J}\, \tilde{\gamma}$$

where $\lambda^2 \mathbf{I}\, \tilde{\gamma}$ is the overlap part and $(\mu_1^2 + \mu_2^2)\, \mathbf{J}\, \tilde{\gamma}$ is the quadrupole part.

ACKNOWLEDGMENTS

The author is greatly indebted to Professor S. P. Reddy, who supervised the research work presented in this thesis, for his constant interest and valuable advice and for his assistance in the preparation of the thesis material.

Grateful acknowledgment is also due to Professor S. W. Breckon for his continued interest in this research.

The financial assistance received from the National Research Council's operating grant A-2440 is gratefully acknowledged.

The author also appreciates the use of the computer facilities and the assistance of the staff of Technical Services of Memorial University.

The stimulating discussions with Messrs. W. F. Lee and S. G. Lagu proved valuable to the author and are gratefully acknowledged.

Thanks are also due to the faculty and graduate students in the Molecular Physics Section of the Physics Department and to Messrs. R. B. Bishop and A. James for their assistance in the preparation of some of the diagrams used in this thesis.

REFERENCES

1) American Institute of Physics Handbook, 1963.

2) Chisholm, D. A. 1952. Ph.D. Thesis, University of Toronto.

3) Chisholm, D. A. and Welsh, H.L. 1954. Can. J. Phys. 32, 291.

4) Cho, C. W., Allin, E. J. and Welsh, H. L. 1963. Can. J. Phys. 41, 1991.

5) Condon, E. V. 1932. Phys. Rev. 41, 759.

6) Crawford, M. F., Welsh, H. L. and Locke, J. L. 1949. Phys. Rev. 75, 1607.

7) Dean, J. W. 1961. NBS Technical Note 120.

8) De Groot, S. R. and ten Seldam, C. A. 1947. Physica, 13, 47.

9) Hare, W. F. J. and Welsh, H. L. 1958. Can. J. Phys. 36, 88.

10) Hirschfelder, J. L., Curtiss, F. C. and Bird, R. B. 1954. Molecular Theory of Gases and Liquids (Wiley, New York).

11) Kolos, W. and Rothaar, C. C. J. 1960. Rev. Mod. Phys. 32, 219.

12) Lee, W. F. 1967. Thesis, Memorial University of Newfoundland.

13) Mann, D. B. 1962. NBS Technical Note 154.

14) Michels, A., de Boer, J. and Bijl, A. 1937. Physica, 4, 981.

15) Michels, A. and Goudeket, M. 1941. Physica, 8, 347.

16) Michels, A., Graff, W., De Wassenaar, T., Levelt, J. M. H. and Louwerse, P. 1959. Physica, 25, 28.

17) Michels, A., Wassenaar, T. and Louwerse, P. 1960. Physica, 26, 539.

18) Pai, S. T., Reddy, S. P., and Cho, C. W. 1966. Can. J. Phys. 44, 2893.

19) Pai, S. T. 1965. Thesis, Memorial University of Newfoundland.

20) Poll, J. D. 1960. Ph.D. Thesis, University of Toronto, Toronto, Ontario.

21) Racah, G. 1942. Phys. Rev. 61, 186; 1942. Phys. Rev. 62, 438; 1943, Phys. Rev. 63, 968.

22) Reddy, S. P. and Cho, C. W. 1965a. Can. J. Phys. 43, 793.

23) Reddy, S. P. and Cho, C. W. 1965b. Can. J. Phys. 43, 2331.

24) Reddy, S. P. and Lee, W. F. 1968 Can. J. Phys. (in press).

25) Sinha, B. B. P. 1967. Thesis, Memorial University of Newfoundland.

26) Timmerhaus, K. D. 1963. Advances in Cryogenic Engineering, Plenum Press, New York, Vol. 8, 135-145.

27) Thomson, H. W. 1961. I.U.P.A.C. Tables of Wavenumbers.

28) Van Kranendonk, J. 1957. Physica, 23, 825.

29) Van Kranendonk, J. 1958. Physica, 24, 347.

30) Van Kranendonk, J. and Bird, R. B. 1951. Physica, 17, 953 and 968.

31) Van Kranendonk, J. 1959. Physica, 25, 1080.

32) Van Kranendonk, J. and Kiss, Z. J. 1959. Can. J. Phys. 37, 1187.

33) Watanabe, A., and Welsh, H. L. 1965. Can. J. Phys. 43, 818.

34) Woolley, H. W., Scott, R. B. and Brickwedde, F. G. 1948. J. Res. Nat. Bur. Std., 41, 396-434.